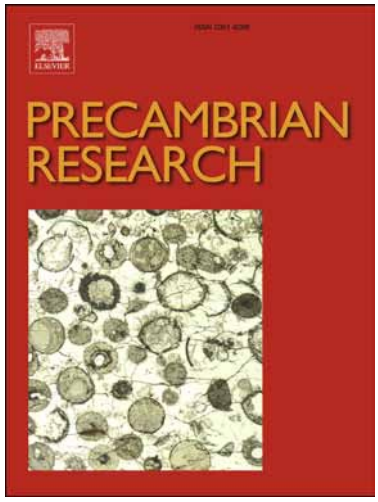

Reconstructing Cryogenian to Ediacaran successions and paleogeography of the South China Block

Liang Qi, Yajun Xu, Peter A. Cawood, Yuansheng Du

PII: S0301-9268(18)30072-X
DOI: https://doi.org/10.1016/j.precamres.2018.07.003
Reference: PRECAM 5123

To appear in: *Precambrian Research*

Received Date: 1 February 2018
Revised Date: 4 July 2018
Accepted Date: 6 July 2018

Please cite this article as: L. Qi, Y. Xu, P.A. Cawood, Y. Du, Reconstructing Cryogenian to Ediacaran successions and paleogeography of the South China Block, *Precambrian Research* (2018), doi: https://doi.org/10.1016/j.precamres.2018.07.003

Reconstructing Cryogenian to Ediacaran successions and paleogeography of the South China Block

Liang Qi[1,2], Yajun Xu[1,2,*], Peter A. Cawood [3, 4], Yuansheng Du[1,2]

[1.] *State Key Laboratory of Geological Processes and Mineral Resources, Center for Global Tectonics, School of Earth Sciences, China University of Geosciences, Wuhan, 430074, China*

[2.] *State Key Laboratory of Biogeology and Environmental Geology, School of Earth Sciences, China University of Geosciences, Wuhan, 430074, China*

[3.] *School of Earth, Atmosphere & Environment, Monash University, Melbourne, VIC 3800, Australia*

[4.] *Department of Earth Sciences, University of St. Andrews, North Street, St. Andrews KY16 9AL, UK*

* Corresponding author: xuyajun19@163.com (Yajun Xu)

Tel: +86 27 67883001, Fax: +86 27 67883002

Abstract

Neoproterozoic paleogeography of the South China is dominated by the formation of Rodinia, its break-up, and the subsequent amalgamation of Gondwana. Two negative excursions of the chemical index of alteration (CIA) and the chemical index of weathering (CIW) recorded in the Cryogenian to Ediacaran sedimentary rocks of the Cathaysia Block, South China, indicate two cooling events. In combination with available age constraints, this data suggests correlation with the global Marinoan (ca. 650-635 Ma) and Gaskiers (ca. 579 Ma) glaciations. U-Pb ages of detrital zircons from the Cryogenian to lower Ediacaran strata define two distinctive age peaks at 1056 Ma and 998 Ma, whereas the upper Ediacaran strata show only one age peak at 957 Ma. These data demonstrate Neoproterozoic sedimentary rocks in the Cathaysia Block were derived from a source external to the craton. The predominant late Mesoproterozoic to early Neoproterozoic (1140-870 Ma) detrital zircons were most likely derived from a source dominated by North India and East Antarctica with limited input from Western Australia. Furthermore, $\varepsilon_{Hf}(t)$ values of detrital zircons are similar to the coeval detrital zircons from Rayner-Eastern Ghats. The detrital record of the late Cryogenian and Ediacaran strata in the Cathaysia Block suggests that the South China Block was connected to the northern margin of India during the dispersal of Rodinia and the assembly of East Gondwana. Detrital zircons from Cryogenian strata overlying the Jiangnan Orogen are largely in the range 900-700 Ma with scattered Archean and Paleoproterozoic grains. These ages are consistent with derivation from local sources within South China. The timing of accumulation of these units, after collisional assembly of South China, likely accounts for their more restricted provenance with collision generated relief providing both a local source and restricting input from further south within India and/or the rest of Gondwana.

Keywords: **South China; Neoproterozoic; Rodinia; Gondwana; Detrital zircon; North India**

1. Introduction

Tectonic and paleogeographic models for the South China Block agree that by the early Paleozoic the constituent Yangtze and Cathaysia blocks were amalgamated along the intervening Jiangnan Orogen, and that it was joined to northern India along the northern margin of East Gondwana (Xu et al., 2013; Yao et al., 2014; Wang et al., 2010). However, its Neoproterozoic history is disputed with one set of models arguing that it had been linked to India since at least the mid-Neoproterozoic and probably earlier (Cawood et al., 2013, 2018; Charvet, 2013; Merdith et al., 2017; Yu et al., 2008; Zhao and Cawood, 2012), whereas others suggest it was only accreted to northern Gondwana at the end of the Neoproterozoic (Li et al., 2003; Li et al., 2008; Li et al., 2002b; Wang et al., 2010; 2014). Key to resolving these models is the provenance of Neoproterozoic sedimentary rocks in South China.

Provenance and paleocurrent data for early Paleozoic strata in South China indicate input from a source beyond the craton within Gondwana, which included northeast India and Western Australia/Antarctica (Cawood et al., 2013, 2018; Wang et al., 2010; Xu et al., 2013, 2014a; Yu et al., 2008). If South China was linked to India in the Neoproterozoic, then strata of this age should also show input from external sources. Alternatively, those models advocating an allochthonous origin and subsequent accretion of South China to India suggest it occupied a separate plate prior to collision and hence Neoproterozoic strata should indicate derivation from a local sources within the craton. In this paper, we provide a new evidence to constrain the depositional age of Cryogenian and Ediacaran strata that overlie the Cathaysia Block, and investigate the provenance of Neoproterozoic siliciclastic rocks in the southern South China Block in order to demonstrate a similar source to early Paleozoic strata. These results indicate that the craton was joined to India throughout this timeframe. In addition, we provide evidence for glacial influenced weathering during accumulation of

Ediacaran strata overlying the Jiangnan Orogen and Cathaysia Block.

2. Geological Setting

The South China Block consists of the Yangtze Block to the northwest and the Cathaysia Block to the southeast separated by the Jiangnan Orogen (Fig. 1). Prior to the Neoproterozoic, the Yangtze and Cathaysia blocks experienced independent histories (Shu, 2006; Zhao and Cawood, 2012). The Yangtze Block consists of Archean-Paleoproterozoic crystalline basement surrounded by early Neoproterozoic fold belts. The oldest exposed rocks are Archean granitic gneiss (3.45-3.2 Ga) in the Kongling area with two stage Hf model ages for zircons in the range of 3.9-3.6 Ga (Guo et al., 2014; Gao et al., 1999). The oldest exposed rocks in the Cathaysia Block constitute the Paleoproterozoic Badu Complex (1.8-1.9 Ga, Chen et al.,2016; Liu et al., 2009; Yu et al., 2012; Yu et al., 2009), which sporadically crop out in the Wuyi region (Wan et al., 2007; Zhao and Cawood, 2012). The presence of Archean zircons in Phanerozoic granites and late Neoproterozoic-early Paleozoic strata, some with ages as old as 4.1 Ga (Xing et al., 2014; Zhang et al., 2006; Xu et al., 2013; Yu et al., 2007), suggest that the block is either underlain by, or lay adjacent to, Archean crust.

The Yangtze and Cathaysia blocks amalgamated during the early to mid-Neoproterozoic along the Jiangnan Orogen (Fig. 1; Zhao and Cawood, 1999; Cawood et al., 2013; Wang et al., 2013a; Li et al., 2018; Yao et al., 2015). The unified craton is overlain by a middle to upper Neoproterozoic succession that is inferred to have accumulated in a failed rift environment (i.e. Nanhua and Kangdian rifts) (Shu et al., 2008a, 2011; Wang et al., 2003; Zhao and Cawood, 2012). Lower Paleozoic strata conformably overlie the Precambrian succession and show significant facies variation across the craton with the Cambrian-Ordovician succession ranging from graptolite-bearing siliciclastic rocks in the Cathaysia Block to a mixed carbonate, siliciclastic succession in the region of the Jiangnan Orogen and a carbonate succession that represents a platform environment in the Yangtze Block (Shu et al., 2014; Wang et al., 2010).

Early Paleozoic and older rock units in the Cathaysia Block experienced an extensive tectonothermal event during the mid-Paleozoic (Li et al., 2009; Wang et al., 2012b; Wang et al., 2011; Wang et al., 2014b; Xu et al., 2016; Xu et al., 2014a).

3. Stratigraphy and Samples

Upper Neoproterozoic strata in South China are well preserved in the region of the Jiangnan Orogen and in the Wuyi-Nanling-Yunkai region of the Cathaysia Block (Fig. 1). Radiometric dating on tuffaceous siltstone indicates the sedimentary succession ranges in age from early Cryogenian (716 ± 2.8 Ma, Lan et al., 2015) to late Ediacaran (551 ± 0.7 Ma, Condon et al., 2005). Lithostratigraphic relations through the Cryogenian and Ediacaran succession are shown in figure 2, including formation names, lithologies, thicknesses and inferred correlations in the study regions. The oldest units are unconformable on the Jiangnan Orogen and Cathaysia Block, accumulating after their assembly and pass conformably up into early Paleozoic strata (BGMRFP, 1985).

Twelve samples were collected through the Cryogenian and Ediacaran succession for detrital zircon age analysis and sixty-nine samples for whole rock geochemical analysis (Figs. 2, 3). Three detrital zircon samples are from the Cryogenian succession overlying the Jiangnan orogen. Samples 15JP-31 and 15JP-32 are from the Liangjiehe Formation and are white gravelly claystones, containing oval shaped quartz grains ranging in size from 0.1 cm to 0.5 cm. Sample SJ-B-2 is a violet-colored siltstone from the Datangpo Formation. A further three zircon samples were collected from sandstones of the Xiafang Formation (16ZT-12) and the Louziba Formation (15CT-89, 15CT-84) in the region of the Cathaysia Block. In addition, 6 zircon samples were collected from the Ediacaran units in the Cathaysia Block. Sample 16NX-13 from the Laohutang Formation in the Nanxiong area, 15CT-76 from the Nanyan Formation, 15CT-66 and 15CT-60 from the Huanglian Formation, and PM02-4 and PM02-17 from the Xixi Formation in the Changting area (Figs. 2, 3). The sandstones are grey to

pale-green and fine grained. Lithic fragments include granite, polycrystalline quartz, and metamorphic and sedimentary rock fragments.

Forty nine samples were collected for whole-rock geochemical analysis from a traverse through the Louziba, Nanyan and Huanglian formations in the southwestern Changting area with a further twenty samples from the Xixi Formation in the northern Changting area (Fig. 3).

The Ediacaran succession overlying the Jiangnan Orogen is mostly composed of carbonate and is unsuitable for detrital zircon and whole rock geochemical analysis.

4. Analytical Methods

4.1 LA-ICMPS U-Pb dating of detrital zircons

Zircons were separated by conventional heavy liquid and magnetic techniques. Grains were selected under a binocular microscope at the Langfang Regional Geophysical Survey, Hebei Province, China. Zircons are mounted in epoxy resin, sectioned and polished approximately in half, and imaged in transmitted light and by cathodoluminescence (CL) at the Beijing GeoAnalysis Co., Ltd. U-Pb dating analyses of zircon were conducted on an Agilent 7500a laser inductively coupled plasma mass spectrometer (LA-ICP-MS) at the State Key Laboratory of Geological Processes and Mineral Resources, China University of Geosciences in Wuhan. Laser sampling was performed using an excimer laser ablation system (GeoLas 2005). Detailed operating conditions and data reduction methodologies are described by Liu et al. (2010). Off-line selection of the background and analytic integrations, as well as instrument drift correction and quantitative calibration for the U-Pb dating, were performed using ICPMSDateCal (Liu et al., 2010; Liu et al., 2008). Zircon 91500 was used as the calibration standard for U-Pb dating and was analyzed twice every seven analyses. Time-dependent drift of U-Th-Pb isotopic ratios were corrected using a linear interpolation (with time) for every seven analyses according to the variations of 91500 (Liu et al., 2010). GJ-1 was analyzed as an unknown. Our

measurements of 91500 and GJ-1 yielded weighted mean $^{206}Pb/^{238}U$ ages of 1062.4 ± 1.4 Ma (2 σ, MSWD = 0.05, n = 265) and 595.6 ± 3.1 (2 σ, MSWD = 2.8, n = 79), respectively, which are in good agreement with the measured isotope dilution thermal ionization mass spectrometry (ID-TIMS) $^{206}Pb/^{238}U$ ages of 1062.4 ± 0.4 and 598.5-602.7 Ma (2 σ) (Jackson et al., 2004). Concordia diagrams and weighted mean calculations were made using Isoplot/Ex_ver3 (Ludwig, 2003). Common Pb correction was not performed as the measured ^{204}Pb signal is low and U-Pb ages are concordant or nearly concordant.

4.2 In-situ Lu-Hf isotope analysis of detrital zircons

Zircon Hf isotope analyses were carried out in situ using a Neptune Plus MC-ICP-MS (Thermo Fisher Scientific, Germany) in combination with a Geolas 2005 excimer ArF laser ablation system (Lambda Physik, Göttingen, Germany) at the State Key Laboratory of Geological Processes and Mineral Resources, China University of Geosciences in Wuhan. The energy density of laser ablation was 5.3 J cm^2. A "wire" signal smoothing device is included in this laser ablation system, by which smooth signals are produced even at very low laser repetition rates down to 1 Hz (Hu et al., 2012). More details on analytical and calibration procedures can be found in Hu et al. (2012). Analytical spots were located close to LA-ICP-MS spots, or in the same growth domain as inferred from CL images. Reference zircons 91500 and GJ-1 were used to monitor accuracy of interference correction during Hf analysis. Zircon 91500 yielded a $^{176}Hf/^{177}Hf$ ratio 0.2823084 ± 0.000007 (n = 20, 1 σ) compared to the recommended value of 0.282308 ± 6 (Blichert-Toft, 2008), and 0.282002 ± 0.000011 (n = 6, 1 σ) for GJ-1 compared to the recommended value of 0.282015 ± 19 (Elhlou et al., 2006). The $^{179}Hf/^{177}Hf$ and $^{173}Yb/^{171}Yb$ ratios were used to calculate the mass bias of Hf (β_{Hf}) and Yb (β_{Yb}), which were normalized to $^{179}Hf/^{177}Hf = 0.7325$ and $^{173}Yb/^{171}Yb = 1.132685$ (Fisher et al., 2014) using an exponential correction for mass bias. Interference of ^{176}Yb on ^{176}Hf was corrected by measuring the interference-free ^{173}Yb isotope and using $^{176}Yb/^{173}Yb = 0.79639$ (Fisher et al., 2014) to calculate $^{176}Yb/^{177}Hf$.

4.3 Whole-rock major elements

Fresh rock samples were cleaned with deionized water, and subsequently crushed and powdered with an agate mill. The major elements of samples were determined using the ME-XRF26d methods, at the ALS Chemex Company of Guangzhou, China. Supplementary Data Table S3 lists the chemical compositions of 69 samples. The prepared samples were fused with a lithium tetraborate ($Li_2B_4O_{7)}$ and lithium metaborate ($LiBO_2$) flux and then fused to a glass bead at 1050-1100°C in an automatic melting instrument. The resultant disk was then analyzed using X-ray fluorescence spectrometry (XRF) for major elements. The analysis accuracy was < 2% and the detection limits are < 0.01%.

5. Results

5.1. Zircon Morphology

Zircons are colorless with oscillatory zoning and some show core-rim structures under CL. Zircons preserved in the Cryogenian samples 15JP-31,15JP-32 and SJ-B-2 overlying the Jiangnan Orogen are euhedral to subhedral, and the lengths of grains range from 70 μm to 180 μm (most around 100 μm), with aspect ratios of 1:1 to 3:1. The euhedral grains suggest little or only short distance transport. Zircons from late Cryogenian to Ediacaran samples PM02-4, PM02-17, 15CT-89, 15CT-84, 15CT-76, 15CT-66, 15CT-60, 16ZT-12 and 16NX-13 overlying the Cathaysia Block are subhedral to oval crystals or crystal fragments. Grains range in length from 30 μm to 150 μm (most around 80 μm) with aspect ratios of 1:1 to 2:1. The oval shaped grains suggest prolonged, and possibly multicycle, transport.

In addition to oscillatory zoning, the Th/U ratios of the zircons range from 0.1 to 9.33, consistent with a magmatic origin (Belousova et al., 2002). A few grains in both Jiangnan Orogen, with ages ranging from 1189 to 809 Ma, and Cathaysia Block with ages ranging from 2489 to 2256 Ma and 1206 to 928 Ma, display homogeneous internal structures and have low Th/U ratios. Cathodoluminescence (CL) images of representative zircons are presented in

figure 4.

5.2. Detrital Zircon U-Pb Ages

A total of 929 analyses of 927 zircons were undertaken from 12 samples from the Neoproterozoic strata on the South China Block. Most analyses are located in the core region of grains with only a few analyses from the margin of grains. Zircon U-Pb isotopic compositions are presented in Supplementary Data Table S1. Uncertainties on individual analyses in the data table and concordia plots are presented at 1 σ. All analyses are shown on concordia plots (Fig. 5), however analyses with greater than 10% discordance are not included in frequency diagrams (Fig. 6), and ages less than 1000 Ma are based on the $^{206}Pb/^{238}U$ ratio whereas older ages are based on the $^{206}Pb/^{207}Pb$ ratio. Ages calculated for multiple grains are quoted with 95 % confidence limits.

In sample 15JP-32, 68 of 75 analyses plot on or near concordia and yielded ages ranging from 1.49 Ga to 0.68 Ga. Age spectra can be classified into three groups, with the oldest zircon yielding a $^{207}Pb/^{206}Pb$ age of 1498 ± 91 Ma, 27 analyses ranging from 0.95 Ga to 0.83 Ga, and 39 analyses from 0.82 Ga to 0.68 Ga. Two dominant peaks occur at 905 ± 8 Ma (MSWD = 0.73, n = 14) and 786 ± 6 Ma (MSWD = 0.76, n = 16).

Seventy analyses were determined from 15JP-31, of which 60 were within 10% of concordia. Analyses fall into two age groups: three analyses are distributed between 2.0 and 1.9 Ga, and 57 analyses form a group between 0.95 and 0.70 Ga with a single age peak at 802 ±6 Ma (MSWD = 0.64, n = 18).

For sample SJ-B-2, 71 of 72 analyses of zircons are concordant, and are divided into four major age ranges: two analyses are scattered along concordia between 2.88-2.70 Ga, eight analyses are evenly distributed between 2.55 and 2.30 Ga, 11 fall between 2.07 and 1.80 Ga, and 50 analyses range from 1.02 to 0.65 Ga. The latter define a main peak at 801 ± 5 Ma (MSWD = 0.81, n = 21) whereas the Paleoproterozoic grains are distributed about a subordinate peak at 1892 ± 76 Ma (MSWD = 0.45, n = 5).

Of 87 analyses from sample 16ZT-12, 85 display 90% or greater concordance and yield ages ranging from 2.57 to 0.62 Ga. Age spectra can be classified into five groups, including four analyses scattered along concordia between 2.57-2.30 Ga, six analyses ranging from 2.06 to 1.96 Ga, four analyses that form a tight group from 1.58 Ga to 1.51 Ga, a group of analyses fall in the interval between 1.35 and 0.89 Ga, and the youngest group of analyses from 0.80-0.63 Ga. Two dominant age peaks occur at 1076 ± 40 Ma (MSWD = 1.26, n = 23) and 976 ± 8 Ma (MSWD = 1.2, n = 9), with three subordinate peaks at 2023 ± 81 Ma (MSWD = 1.8, n = 6), 1542 ± 75 Ma (MSWD = 1.5, n = 4), and 640 ± 12 Ma (MSWD = 0.25, n = 2).

Eighty seven grains were analyzed from sample 16NX-13 and yielded 78 ages within 10% of concordia, which fall in the range of 3.11 to 0.55 Ga Ga. Age spectra can be classified into five groups: 3.11 to 2.94 Ga, 2.66 to 2.27 Ga, 1.96 to 1.67 Ga, 1.42 to 0.72 Ga and the two youngest grains, which yielded concordant ages of 558 ± 12 Ma (90%) and 551 ± 8 Ma (99%). Two dominant peaks occur at 960 ± 7 Ma (MSWD = 0.98, n = 11) and 764 ± 8 Ma (MSWD = 1.07, n = 7) and four subordinate peaks at 2457 ± 29 Ma (MSWD = 0.56, n = 7), 1716 ± 38 Ma (MSWD = 0.76, n = 5), 1094 ± 50 Ma (MSWD = 1.2, n = 7), and 551 ± 13 Ma (MSWD = 0.01, n = 2).

For sample 15CT-89, 81 of 87 analyzed zircon grains are greater than 90% concordant, and yielded ages ranging from 4.21 Ga to 0.64 Ga. The oldest zircon yielded a $^{207}Pb/^{206}Pb$ age of 4219 ± 85 Ma, with concordance of 96% (Fig. 4a), which is the oldest material recorded from the South China Block. Other analyses are grouped into four major age ranges: 2.83 to 2.50 Ga, 2.37 to 1.75 Ga, 1.58 to 0.94 Ga and 0.87 to 0.64 Ga, with two dominant peaks at 1055 ± 13 Ma (MSWD = 3.1, n = 16) and 964 ± 21 Ma (MSWD = 3.7, n = 9), and three subordinate peaks at 2279 ± 79 Ma (MSWD = 2.1, n = 4), 1836 ± 31 Ma (MSWD = 1.2, n = 6), 648 ± 12 Ma (MSWD = 0.28, n = 3).

Analyses of 68 of 71 zircons from 15CT-84 display 90% or greater concordance, yielding ages ranging from 2.75 to 0.66 Ga, and fall into five major

age groupings: 2.7 to 2.35 Ga, 2.19 to 1.88 Ga, 1.48 to 1.23 Ga, 1.17 to 0.93 Ga and 0.88 to 0.66 Ga. Two dominant peaks at 1089 ± 14 Ma (MSWD = 2.4, n = 15) and 999 ± 7 Ma (MSWD = 0.59, n = 9), and three subordinate peaks at 2584 ± 88 Ma (MSWD = 2.2, n = 4), 1338 ± 47 Ma (MSWD = 0.55, n = 5), and 871 ± 50 Ma (MSWD = 2.5, n = 3).

Zircons in 15CT-76 yielded ages ranging from 2.37 to 0.61 Ga on 71 grains of which 70 were within 10% of concordia. Age spectra can be classified into four groups: 2.37 to 2.18 Ga, 1.75 to 1.43 Ga, 1.34 to 0.90 Ga, 0.82 to 0.70 Ga and 0.66 to 0.61 Ga, with two dominant peaks at 1038 ± 40 Ma (MSWD = 1.8, n = 22), 1122 ± 22 Ma (MSWD = 0.88, n = 15) and one subordinate peak at 705 ± 13 Ma (MSWD = 0.06, n = 3).

For 15CT-66, 65 of 71 analyzed zircon grains are greater than 90% concordant, and seven groups of analyses can be distinguished in the interval between 2.75 and 0.54 Ga: 2.88 to 2.78 Ga, 2.58 to 2.32 Ga, 1.98 to 1.74 Ga, 1.52 to 1.24 Ga, 1.16 to 0.89 Ga, 0.85 to 0.72 Ga and 0.60 to 0.54 Ga. One dominant peak at 954 ± 10 Ma (MSWD = 0.45, n = 7) and two subordinate peaks at 2416 ± 55 Ma (MSWD = 2.2, n = 7), 772 ± 12 Ma (MSWD = 0.44, n = 4).

Analyses of 64 of 74 zircons from 15CT-60 show more than 90% concordance and are scattered between 2.96 and 0.74 Ga. Age spectra can be classified into six groups: 2.96 to 2.63 Ga, 2.44 to 2.26 Ga, 2.18 to 1.69 Ga, 1.50 to 1.37 Ga, 1.32 to 0.86 Ga and 0.79 to 0.64 Ga, with one dominant peak at 957 ± 8Ma (MSWD = 1.8, n = 23), and three subordinate peaks at 1501 ± 54 Ma (MSWD = 2.1, n = 6), 1088 ± 9 Ma (MSWD = 1.9, n = 24), and 708 ± 14 Ma (MSWD = 0.39, n = 2).

For PM02-4, 69 of 71 analyzed zircon grains are greater than 90% concordant, and yielded ages ranging from 2.74 Ga to 0.63 Ga. Analyses are grouped into four major age ranges: 2.74 to 2.47 Ga, 2.08 to 1.74 Ga, 1.58 to 0.90 Ga and 0.87 to 0.63 Ga, with one dominant peak at 987 ± 9 Ma (MSWD = 0.53, n = 21), and three subordinate peaks at 1134 ± 29 Ma (MSWD = 0.66, n = 14), 1504 ± 51 Ma (MSWD = 1.4, n = 8), and 681 ± 13 Ma (MSWD = 0.12, n = 4).

All 71 zircon grains analyzed from sample PM02-17 display 90% or greater concordance and yield ages ranging from 2.40 to 0.62 Ga. Analyses fall into five major age ranges: 2.4 to 1.91 Ga, 1.63 to 1.52 Ga, 1.38 to 0.93 Ga and 0.89 to 0.62 Ga. One dominant peak at 993 ± 9 Ma (MSWD = 0.51, n = 16), and three subordinate peaks at 1128 ± 39 Ma (MSWD = 1.3, n = 8), 1368 ± 34 Ma (MSWD = 0.14, n = 4), and 1550 ± 43 Ma (MSWD = 0.44, n = 4).

5.3. Zircon Hf Isotope Compositions

Hf isotope compositions were analyzed on 67 zircons from samples SJ-B-2 and 15CT-76 (Supplementary Data Table S2). Analyzed grains all had U-Pb ages with greater than 95% concordance (Fig. 7).

Zircons in SJ-B-2 with crystallization age of 0.83 Ga to 0.78 Ga exhibit a range of $\varepsilon_{Hf}(t)$ values from -18.9 to 10.6, with model ages from 2.62 Ga to 0.98 Ga. The predominant ca. 800 Ma zircon grains are characterized by variable $\varepsilon_{Hf}(t)$ values, with the more positive values suggest derivation mainly from juvenile crust.

Zircons in 15CT-76, with crystallization ages of 1.17 Ga to 0.91 Ga, exhibit a large range of $\varepsilon_{Hf}(t)$ values from to -10.9 to 11.0 , with model ages from 2.37 Ga to 1.19 Ga. The predominant ca. 1000 Ma zircon grains are characterized by variable $\varepsilon_{Hf}(t)$ values, but the more negative values indicate derivation mainly from reworking of older crustal components.

5.4 Major elements

The whole-rock major elements compositions of 69 samples are presented in Supplementary Data Table S3. The major-element geochemistry of siliciclastic sedimentary rocks are strongly affected by chemical weathering, mineral sorting and post-depositional alteration. Chemical weathering leaches and subsequently depletes the soluble elements Ca, Na, and K relative to refractory element Al, and forms Al-bearing clay minerals in the residual materials. Therefore, the chemical index of alteration (CIA) values, chemical index of weathering (CIW) and the

index of variability (ICV) provide a record of the intensity of chemical weathering and associated climate conditions. To minimize the impact on CIA alteration values from sorting process during transportation and deposition, only fine-grained samples were chosen for paleoclimate discussion, avoiding medium to coarse-grained siliciclastic sedimentary rocks (Fedo et al., 1995).

Fine grained siliciclastic rocks from the Louziba, Nanyan, Huanglian and Xixi formations contain variable contents of Al_2O_3, K_2O, CaO, Na_2O, Fe_2O_3, MgO and TiO_2, which lead to variable CIA and CIW values. Al_2O_3 content displays an inverse correlation with SiO_2 (r = -0.97). The lowest SiO_2 contents are observed in mudstones from the Nanyan, Huanglian and Xixi formations. Other major element oxides, such as MnO, P_2O_5 and BaO, do not show any significant trend and overall concentrations are low. The CIA and CIW values show significant stratigraphic variations through the succession including two pronounced negative excursions (NE1 and NE2, Fig. 8). The first negative excursion (NE1) is established from 11 samples from the Louziba Formation which show similar low CIA (64.09-77.71, average 70.34) and CIW values (72.58-95.44, average 83.46), which then progressively increase up stratigraphy toward to the Nanyan Formation. In contrast, CIA and CIW values from the lower to middle Nanyan (CIA 65.72-83.95, average 77.25; CIW 75.25-99.63, average 94.50) and correlative lower Xixi formations (CIA 75.64-81.67, average 78.23; CIW 94.12-99.24, average 98.42) are clearly higher between NE1 and NE2. CIA and CIW values decrease in the upper Nanyan Formation (CIA 63.21-71.76, average 66.61; CIW 72.01-84, average 77.29) and middle Xixi Formation (CIA 64.19; CIW 79.12) relative to the top of the Nanyan Formation and overlying Huanglian Formation (CIA 70.98-80.67, average 75.82; CIW 87.36-99.39, average 95.11), and with respect to the upper Xixi Formation (CIA 70.66-84.13, average 79.34; CIW 81.18-99.46, average 97.29). These low values define negative excursion 2 (NE2).

6. Discussion

6.1 Depositional age of the Neoproterozoic strata

It is difficult to obtain precise and reliable depositional ages of the Neoproterozoic siliciclastic rocks in the Cathaysia Block due to the absence of volcanic interbeds. U-Pb ages of the youngest zircons constrain a maximum depositional age (e.g., Brown and Gehrels, 2007; Dickinson and Gehrels, 2009).

The two youngest zircons from the Louziba Formation generate concordant ages of 646 ± 10 Ma (98%) and 650 ± 8 Ma (98%), respectively. Combining the youngest grains with age of 664 ± 14 Ma reported by Wang et al. (2018) from this unit, we define a weighted mean maximum deposition age of 650 ± 11 Ma (MSWD = 0.56, n = 3) for the Louziba Formation. The upper age limit on the unit is provided by micro-plant fossils, which suggest a pre-Ediacaran age (> 635 Ma, Zhang et al., 2005). Therefore, the Louziba Formation likely accumulated in the Cryogenian between 650-635 Ma and is correlated with the upper Nantuo Formation that overlies the Yangtze Block. (Fig. 9).

The youngest zircon dated in the Nanyan Formation gave a concordant age of 614 ± 10 Ma (94%). Micro-plant fossil acritarchs *Protoleiospharidium* sp., and *Micrhystridium* sp., are preserved in this unit and also occur in Ediacaran strata of South China and Antarctica (Ding et al., 1992; Sarjeant and Stancliffe, 1994; BGMRFP, 1985; Zhang et al., 2005). This indicates that the Nanyan Formation probably accumulated in the Ediacaran and is likely contemporaneous with Doushantuo Formation overlying the Jiangnan Orogen (Fig. 9).

The youngest zircon analyzed in the Huanglian Formation has a concordant age of 544 ± 9 Ma (90%). Micro-plant fossil sponge spicules *Micrconcentrica* sp., and *Archaeohy strichosphaeridium* sp. are very different from those preserved in the overlying Cambrian sequences in the study area (BGMRFP, 1985; Zhang et al., 2005), but similar to those found in the Ediacaran strata of the northeastern Lesser Himalaya (Shukla M et al., 2005; Tewari, 2001). These data suggest that the Huanglian Formation accumulated in the latest Ediacaran and is contemporaneous with the Dengying/Laobao Formation that overlies the Yangtze Block (Fig. 9).

The youngest zircon from the Xixi Formation has a concordant age of 636 ± 11 Ma (99%). Micro-fossil acritarchs *Micurhystridium* sp., and *Leiominuscula* sp. are found in Xixi, Doushantuo and Dengying formations (BGMRFP, 1985), which suggests that Xixi Formation was probably deposited in the late Neoproterozoic.

Two youngest zircons from the Xiafang Formation yield a weighted mean age of 640 ± 12 Ma (MSWD = 0.25, n = 2). This age suggests that the Xiafang Formation may be consistent with regional correlations of the unit with the Louziba Formation in the southern Wuyi region (BGMRGP, 1988).

Two youngest zircons from the Laohutang Formation have a weighted mean age of 551 ± 13 Ma (MSWD = 0.01, n = 2), close to the boundary of the Doushantuo and Dengying formations (551 ± 0.7 Ma, Condon et al., 2005). The Laohutang Formation contains the micro-plant fossils Chlorophya *protoleiosphaeridium* sp., and *Leiopso - phosphaera pelucidus* (BGMRGP, 1988), which are also found in Ediacaran strata elsewhere in South China and in Antarctica (Thomson, 1977; Yin, 1986; Liu et al., 1984), indicating the formation was deposited in the late Ediacaran and is equivalent to the Huanglian Formation in southern Wuyi region (BGMRGP, 1988).

Deposition ages of the late Neoproterozoic successions overlying the Jiangnan Orogen have been constrained by precise U-Pb ages of zircons from tuff layers within the successions (Fig. 9; Lan et al., 2015; Lan et al., 2014; Zhang et al., 2008; Zhou et al., 2004). Youngest detrital zircon ages from the analyzed samples are consistent with a Cryogenian depositional age. Samples 15JP-31 and 15JP-32 were collected from the Liangjiehe Formation and have youngest detrital zircon with $^{206}Pb/^{238}U$ ages of 708 ± 10 Ma and 679 ± 11 Ma. The youngest zircon from SJ-B-2 from the Datangpo Formation has a $^{206}Pb/^{238}U$ age of 659 ± 11 Ma.

6.2 Chemical weathering trends: new evidence in correlating the Neoproterozoic strata overlying the Cathaysia Block.

The Sturtian (717–660 Ma, Rooney et al., 2015), Marinoan (ca. 650-635 Ma, Bao et al., 2018; Prave et al., 2016; Zhao and Zheng, 2010), and Gaskiers (ca. 579 Ma, Pu et al., 2016; Hoffman and Li, 2009) glaciations are widely recognized in Neoproterozoic successions. In South China, evidence for these glacial events has been limited to central South China (Wang et al., 2017), and no glacial deposits were reported from Neoproterozoic strata overlying the Cathaysia Block.

The Cryogenian is characterized by a glacial and interglacial succession that unconformably overlies rock units of the Jiangnan Orogen (Fig. 9). The succession commences with the Chang'an Formation that is correlated with the Sturtian I glaciation (Lan et al., 2015). The upper part of the Fulu Formation in the western Jiangnan orogen is correlated with the Sturtian II glaciation (Lan et al., 2015), with the Dongshanfeng/Gucheng Formation representing a time-equivalent unit overlying the western-central Jiangnan orogen. The overlying glacial deposits in the Nantuo Formation are equated to the Marinoan glaciation (Liu et al., 2015). Recent data from the Doushantuo Formation indicate a cold water depositional environment related to the ca. 580 Ma Gaskiers glaciation (Wang et al., 2017a).

The late Neoproterozoic sequences in the Wuyi-Nanling region of the Cathaysia Block are characterized by a fine grained sedimentary succession. Glacial diamictites have not been recognized, and the lack of paleomagnetic data and interstratified tuffs have prevented understanding the paleogeographic relationship between the Cathaysia and Yangtze and detailed dating of sediment accumulation. Our detrital zircon U-Pb dating results, in combination with microfossil data, suggest that the depositional ages of late Cryogenian and Ediacaran units on the Cathaysia Block overlap in age with the accumulation of the Marinoan and Gaskiers glaciations further west in South China. Specifically, the Louziba Formation is correlated with Marinoan glaciation and the middle part of Nanyan and Xixi formations are correlated with Gaskiers glaciation.

Chemical weathering data from the analyzed samples are consistent with the accumulation of late Neoproterozoic rock units in the Cathaysia region

overlapping with glacial events. CIA and CIW values from the Louziba, Nanyan, Huanglian and Xixi formations display two negative excursions (NE1 and NE2, Fig. 8). These low CIA (50-70) and CIW (60-80) excursions are consistent with minimal chemical alteration, pointing to a cold-arid climatic condition (Nesbitt and Young, 1982; Fedo et al., 1995). In order to validate this approach and interpretation, it is necessary to access the effects of source area, transportation and sediment conditions. For only when a succession is derived from a source region of uniform composition and under similar sediment routing systems, can the variation of CIA values of sedimentary siliciclastic rocks be used to probe the variation of paleoclimate. Detrital zircon age spectra of the nine Neoproterozoic samples overlying the Cathaysia Block display the same age patterns, which suggest they were derived from the same source. Furthermore, the samples mostly have ICV values higher than 1 (1.80-0.65, average 1.07), suggesting that sediment recycling did not significantly influence the chemical composition of our samples, and that there is limited or no polycyclic reworking. Integrating evidence that the negative CIA excursions within our Cryogenian and Ediacaran succession correspond with periodic cold/arid conditions and our constraints on timing of accumulation of the succession, we propose the following correlations with the glacial cycles. The Louziba Formation likely accumulated between 650 Ma and 635 Ma on the basis of detrital zircon and fossil data, consistent with NE1 equating to the Marinoan glaciation (Fig. 9). The Nanyan Formation accumulated after ~614 Ma suggesting that NE2, which occurs within the upper part of the formation and in the Xixi formation, correlates with the Gaskiers glaciation.

A correlation of the Neoproterozoic sections from Yangtze and Cathaysia blocks is possible using the Marinoan and Gaskiers cooling events. The Nantuo tillite in central South China (Yangtze) and Blaini tillite in India (Lesser Himalaya) were both deposited during the Marinoan Snowball Earth event (Hofmann et al., 2011; Jiang G, 2003). The negative $\delta^{13}C$ excursion and silicified glendonites in the Doushantuo Formation are related to the Gaskiers glaciation

yet evidence for tillites in rocks of this age in South China is sparse. Hence, we suggest that the Louziba, Nanyan, Huanglian formations that overlie the Cathaysia Block are correlated with the Nantuo, Doushantuo and Dengying/Laobao formations on the Yangtze Block.

6.3 Sedimentary sources

Detrital zircon age spectra of the nine Neoproterozoic samples overlying the Cathaysia Block display age patterns distinct from the three samples that accumulated on the Jiangnan Orogen (Fig. 10a). The latter group of samples are dominated by detrital zircons with ages between 900-700 Ma with scattered Archean and Paleoproterozoic grains (Fig. 10a). Igneous rocks with ages in the range 900-700 Ma are exposed in the Jiangnan Orogen and adjoining Yangtze and Cathaysia blocks, and record the amalgamation of South China Block (1000-825 Ma), subduction along the western Panxi-Hannan arc system (950-730 Ma), and extension associated with development of the Nahua rift (825-700 Ma; Cui et al., 2017; Li et al., 2018; Li et al., 2005; Wang et al., 2003, 2012a; Xin et al., 2017). Hf isotope data of detrital zircons from sample SJ-B-2 match well those of zircons from igneous rocks within the Jiangnan orogen (Fig. 7), which is further evidence for a local intra-cratonic source. Combined with the angular or euhedral form of the analyzed zircon crystals (Fig. 4), we suggest short distance transport from early Neoproterozoic igneous source rocks within the craton (Wang et al., 2006; Wang et al., 2012a; Li, 1999; Zhou et al., 2009; Han et al., 2016; Hoffman et al., 2001; Wang et al., 2017c). The minor component of older zircon grains with ages of > 1800 Ma were probably derived from Archean and Paleoproterozoic basement elements within the South China.

U-Pb age spectra of nine samples from the Cathaysia Block show a dominant late Mesoproterozoic to early Neoproterozoic age peak clustering around 1140-870 Ma (Fig. 10b). Additional minor peaks occur between 800-540 Ma, and at ca. 1829 Ma and ca. 2412 Ma. In addition, one detrital zircon in sample 15CT-89 has a crystallization age of 4.2 Ga; the oldest material reported

from South China. Early Neoproterozoic igneous rocks crop out in the Wuyi and Yunkai regions of the Cathaysia Block and have zircon U-Pb ages of 997-900 Ma (Fig. 1). Many researchers' suggest that these rocks are closely related to the closure of the earliest Neoproterozoic (ca. 980 Ma) back-arc basin in an accretionary continental margin setting (Zhang et al., 2012b; Wang et al., 2013b, 2014b). Although local detritus with ages between 997 Ma to 900 Ma from a local source cannot be ruled out for our analyzed samples, such a source in unlikely to supply the large amount of subhedral to oval crystals zircon grains with ages between 1140 to 1000 Ma and 700-540 Ma, which are indicative of long distance transport. Hf isotopic compositions of analyzed sample show variable values, which are similar to those from Tethyan Himalaya-India and East Antarctica, but with relatively higher εHf(t) values (> +4) than early Neoproterozoic granitic gneisses in the Cathaysia Block (Fig. 7). These observations suggest a source beyond the South China Block. Rock units with suitable age are widespread in Gondwana (Boger and Miller, 2004; Cawood, 2005; Cawood and Buchan, 2007; Myrow et al., 2010), suggesting the source probably lay within the supercontinent. U-Pb age distributions and Hf isotopic of detrital zircons from the Cryogenian to Ediacaran sequences overlying the Cathaysia Block are similar to those from Greater Himalaya, India and East Antarctica (Fig. 10), but are different from rock units in Western Australia, which have U-Pb age peaks at ca. 1180 Ma and 1650 Ma (Fig. 10). These observations suggest a source region predominantly in North India and East Antarctica with only limited input from Western Australia. Northwest directed paleocurrent data for the Neoproterozoic and early Paleozoic strata overlying the Cathaysia Block (Chen et al., 2006; Shu et al., 2014) also indicate derivation from a source to the southeast. Archean and late Paleoproterozoic detritus were likely also derived from these southern sources, although Paleoproterozoic granites in Cathaysia (Yu et al., 2009, 2012) could also have supplied some detritus.

6.4 Position of South China in Rodinia and Gondwana

The U-Pb age spectra of nine samples from the late Cryogenian and Ediacaran sequences in the Cathaysia Block show that these sedimentary rocks contain abundant late Mesoproterozoic to early Neoproterozoic (1140-870 Ma) and less mid- to late Neoproterozoic (800-540) ages. In general, these are similar to the provenance record of the conformably overlying early Paleozoic strata in South China (e.g., Wang et al., 2010; Xu et al., 2014b), which are consistent with derivation from a southwesterly source within eastern Gondwana (Fig. 11). Five samples from the upper Cryogenian and lower Ediacaran strata have similar age distribution patterns characterized by detritus ranging from 4219 Ma to 614 Ma, with two main age peaks at ca. 1056 Ma and ca. 1002 Ma. The four samples collected from the upper Ediacaran have age distribution patterns with ages ranging from 3112 Ma to 544 Ma, and an age peak at ca. 959 Ma. Thus, prior to 551 Ma, the Cathaysia Block received more detritus from late Mesoproterozoic sources (1100-1000 Ma), whereas after this time it received more early Neoproterozoic (1000-900 Ma) detritus. Potential sources of the late Mesoproterozoic grains are the northern Prince Charles Mountains (1170-1070 Ma, Liu et al., 2017), Rauer Group (1060-1000 Ma, Kinny et al., 1993), Fisher Terrane (1050-1020 Ma, Kinny et al., 1997; Mikhalsky et al., 2002), and Clemence Massif (1100-1040 Ma, Corvino et al., 2005) in Antarctica, whereas the early Neoproterozoic detritus was likely derived from the Eastern Ghats (990-900 Ma) in eastern India (Bhowmik et al., 2012; Boger et al., 2001), the Rayner Complex (990-900 Ma, Dasgupta et al., 2013; Fitzsimons, 2000; Halpin et al., 2005), the Northern Prince Charles Mountains (940-900 Ma, Liu et al., 2016; Morrissey et al., 2015) in northern East Antarctica, and local sources from South China Block. Our $\varepsilon_{Hf}(t)$ values from 15CT-76 also support the Rayner-Eastern Ghats as an important source for the basin (Fig. 7). The evolving source history for the region may reflect the ongoing assembly of the major blocks of Gondwana in the late Neoproterozoic (Collins and Pisarevsky, 2005; Cawood and Buchan 2007) and in particular the assembly between India and Australia/Antarctica along the Kuunga Orogen (570-480 Ma) and its inferred

northern extension towards eastern Cathaysia (Fig. 12; Xu et al., 2014b, 2016).

The change from a local intra-South China source for the Cryogenian strata overlying the Jiangnan Orogen to an external northern Gondwana source in the late Cryogenian to Ediacaran strata overlying the Cathaysia Block need not reflect significant change in the paleogeography of the craton with respect to India. The Cryogenian strata associated with the Jiangnan Orogen immediately postdate early to mid-Neoproterozoic orogenesis associated with assembly of South China. Enhanced relief generated during orogenic thickening would have led to erosion supplying nearby basins within the craton and would have also acted as a barrier to sediment input from further field. Subsidence in the late Cryogenian enabled in input of detritus from sources external to the craton like the northern margin of Gondwana.

7. Conclusions

Integration of new zircon U-Pb-Hf isotopic data and whole-rock geochemical data, with previously published data enables the following conclusions to be drawn on the evolution of the South China Block during the Cryogenian and Ediacaran:

(1) Louziba, Nanyan, Huanglian formations that overlie the Cathaysia Block are correlated with the Nantuo, Doushantuo and Dengying/Laobao formations on the Yangtze Block, and were deposited in the Cryogenian (650-635 Ma), early Ediacaran (635-551Ma) and late Ediacaran (551-541 Ma) respectively. The Xixi Formation was deposited after 636 Ma, and the Xiafang and Laohutang formations, from the Nanxiong area of the Cathaysia Block, were deposited in the Cryogenian (640-635 Ma) and late Ediacaran (551-541 Ma), respectively.

(2) Two climate cooling events can be recognized within late Cryogenian and Ediacaran strata in Cathaysia Block on the basis of chemical weathering data, and likely coincide with the global Marinoan and Gaskiers glaciations.

(3) Cryogenian sequences overlying the Jiangnan Orogen contain euhedral detrital zircons with ages dominantly in the range of 900 Ma to 700 Ma,

consistent with derivation from igneous rocks of this age within the craton.

(4) Detrital zircons from late Cryogenian and Ediacaran samples overlying the Cathaysia Block are rounded and mainly of late Mesoproterozoic to early Neoproterozoic age (1140-870 Ma), suggesting a source beyond the South China Block, and probably from the northern margin of Gondwana.

(5) The overall evolution of the detrital zircon data is consistent with the South China Block being linked to northern India since the Cryogenian.

Acknowledgments

This work was supported by the National Natural Science Foundation of China (Grant No. 41772106 and 41472086) and by the Australian Research Council (Grant FL160100168). We would like to thank Yahui Zang, Liangxuan Jiao, Wei Dai, Hangchuan Zhang and Zukun Zhang from our group and Ciluan Lin from the Regional Geological Survey of Fujian Province for their help during fieldwork. Zhaochu Hu is thanked for their help with zircon U-Pb and Hf isotope analyses. We thank editor Guochun Zhao, associate editor Xianhua Li, and two anonymous reviewers for their comments that led to significant improvements in the manuscript.

References

Belousova, E., Griffin, W., O'Reilly, S.Y., Fisher, N., 2002. Igneous zircon: trace element composition as an indicator of source rock type. Contributions to Mineralogy and Petrology 143, 602-622.

Bhowmik, S.K., Wilde, S.A., Bhandari, A., Pal, T., Pant, N.C., 2012. Growth of the Greater Indian Landmass and its assembly in Rodinia: Geochronological evidence from the Central Indian Tectonic Zone. Gondwana Res. 22, 54-72.

Blichert-Toft, J., 2008. The Hf isotopic composition of zircon reference material 91500. Chemical Geology 253, 252-257.

Bao, X., Zhang, S., Jiang, G., Wu, H., Li, H., Wang, X., An, Z., Yang., T., 2018. Cyclostratigraphic constraints on the duration of the Datangpo Formation and the onset age of the Nantuo (Marinoan) glaciation in South China. Earth. Planet. Sci. Lett. 483, 52-63.

Boger, S.D., Carson, C.J., Wilson, C.J.L., Fanning, C.M., 2000. Neoproterozoic deformation in the northern Prince Charles Mountains, East Antarctica: evidence for a single protracted orogenic event. Precambr. Res. 104, 1-24.

Boger, S.D., Miller, J.M., 2004. Terminal suturing of Gondwana and the onset of the Ross–Delamerian Orogeny: the cause and effect of an Early Cambrian reconfiguration of plate motions. Earth. Planet. Sci. Lett. 219, 35-48.

Boger, S.D., Wilson, C.J.L., Fanning, C.M., 2001. Early Paleozoic tectonism within the East Antarctic craton: The final suture between east and west Gondwana? Geology 29, 463-466.

Brown, E.H., Gehrels, G.E., 2007. Detrital zircon constraints on terrane ages and affinities and timing of orogenic events in the San Juan Islands and North Cascades, Washington. Can. J.. Earth Sci. 44, 1375-1396.

Bureau of Geology and Mineral Resources of Fujian Province (BGMRFP), 1985. Regional Geology of the Fujian Province. Geological Publishing House, Beijing, pp. 1–671 (in Chinese with English abstract)

Bureau of Geology and Mineral Resources of Guangdong Province (BGMRGP), 1988. Regional Geology of the Guangdong Province. Geological Publishing House, Beijing, pp. 1–941 (in Chinese with English abstract).

Bureau of Geology and Mineral Resources of Guangxi Zhuang Autonomous Region (BGMRGZAR), 1985. Regional Geology of the Guangxi Zhuang Autonomous Region. Geological Publishing House, Beijing, pp. 1–853 (in Chinese with English abstract).

Bureau of Geology and Mineral Resources of Guizhou Province (BGMRGP), 1987. Regional Geology of the Guangdong Province. Geological Publishing House, Beijing, pp. 1–698 (in Chinese with English abstract).

Cawood, P.A., 2005. Terra Australis Orogen: Rodinia breakup and development of the Pacific and Iapetus margins of Gondwana during the Neoproterozoic and Paleozoic. Earth-Sci Rev. 69,

249-279.

Cawood, P.A., Buchan, C., 2007. Linking accretionary orogenesis with supercontinent assembly. Earth-Sci Rev. 82: 217-256.

Cawood, P.A., Johnson, M.R.W., Nemchin, A.A., 2007. Early Palaeozoic orogenesis along the Indian margin of Gondwana: Tectonic response to Gondwana assembly. Earth. Planet. Sci. Lett. 255, 70-84.

Cawood, P.A., Wang, Y.J., Xu, Y.J., Zhao, G.C., 2013. Locating South China in Rodinia and Gondwana: A fragment of greater India lithosphere? Geology 41, 903-906.

Cawood, P.A., Zhao, G., Yao, J., Wang, W., Xu, Y., Wang, Y., 2018. Reconstructing South China in Phanerozoic and Precambrian supercontinents. Earth-Sci Rev. In press, at website: https://doi.org/10.1016/j.earscirev.2017.06.001

Charvet, J., 2013. The Neoproterozoic-Early Paleozoic tectonic evolution of the South China Block: An overview. J. Asian Earth Sci.s 74, 198-209.

Chattopadhyay, S., Upadhyay, D., Nanda, J.K., Mezger, K., Pruseth, K.L., Berndt, J., 2015. Proto-India was a part of Rodinia: Evidence from Grenville-age suturing of the Eastern Ghats Province with the Paleoarchean Singhbhum Craton. Precambr. Res. 266, 506-529.

Chen, M.H., Liang, J.C., Zhang, G.L., Li, W.J., 2006. Lithofacies paleogeographic Constraints of southwestern boundary between Yangtze and Cathaysian plates in Caledonian (in Chinese). Geol J. China Univ. 12, 111-122.

Chen, W.T., Sun, W.H., Wang, W., Zhao, J.H., Zhou, M.F., 2014. “Grenvillian” intra-plate mafic magmatism in the southwestern Yangtze Block, SW China. Precambr. Res. 242, 138-153.

Chen, Z.H., Zhao, L., Chen, D.D., Zhao, X.L., Xing, G.F., 2016. First discovery of a Palaeoproterozoic A-type granite in southern Wuyishan terrane, Cathaysia Block: evidence from geochronology, geochemistry, and Nd–Hf–O isotopes. Int. Geol. Rev. 59, 80-93.

Collins, A.S., Pisarevsky, S.A.., 2007. Amalgamating eastern Gondwana: the evolution of the Circum-Indian Orogens. Earth-Sci Rev. 71(3-4): 229-270.

Condon, D., Zhu, M., Bowring, S., Wang, W., Yang, A.H., Jin, Y.G., 2005. U-Pb ages from the neoproterozoic Doushantuo Formation, China. Science 308, 95.

Corvino, A.F., Boger, S.D., Wilson, C.J.L., Fitzsimons, I.C.W., 2005. Geology and SHRIMP U–Pb chronology of the Clemence Massif, central Prince Charles Mountains, East Antarctica. Terra

Antartica. 12, 55–68

Cui, X., Zhu, W.B., Fitzsimons, I.C.W., Wang, X., Lu, Y.Z., Wu, X.H., 2017. A possible transition from island arc to continental arc magmatism in the eastern Jiangnan Orogen, South China: Insights from a Neoproterozoic (870-860 Ma) gabbroic-dioritic complex near the Fuchuan ophiolite. Gondwana Res. 46, 1-16.

Dasgupta, S., Bose, S., Das, K., 2013. Tectonic evolution of the Eastern Ghats Belt, India. Precambr. Res. 227, 247-258.

Dharma Rao, C.V., Santosh, M., Kim, S.W., Li, S., 2013. Arc magmatism in the Delhi Fold Belt: SHRIMP U-Pb zircon ages of granitoids and implications for Neoproterozoic convergent margin tectonics in NW India. J. Asi. Earth Sci. 78, 83-99.

Dickinson, W.R., Gehrels, G.E., 2009. Use of U-Pb ages of detrital zircons to infer maximum depositional ages of strata: A test against a Colorado Plateau Mesozoic database. Earth. Planet. Sci. Lett. 288, 115-125.

Ding, L.F., Li, Y., Chen, H.X., 1992. Discovery of Micrhystridium regulare from Sinian-Cambrain boundary strata In Yichang, Hubei, and its stratigraphic significance. Acta Micropalaeontologica Sinica 9, 303-309.

Elhlou, S., Belousova, E., Griffin W L, Pearson, N.J., S.Y., O.R., 2006. Trace element and isotopic composition of GJ-red zircon standard by laser ablation. Geochimica Et Cosmochimica Acta 70, A158-A158.

Fedo, C.M., Nesbitt, H.W., Young, G.M., 1995. Unraveling the effects of potassium metasomatism in sedimentary rocks and paleosols, with implications for paleoweathering conditions and provenance. Geology 23, 921

Fisher, C.M., Vervoort, J.D., Hanchar, J.M., 2014. Guidelines for reporting zircon Hf isotopic data by LA-MC-ICPMS and potential pitfalls in the interpretation of these data. Chemical Geology 363, 125-133.

Fitzsimons, I.C.W., 2000. Grenville-age basement provinces in East Antarctica: Evidence for three separate collisional orogens. Geology 28, 879-882.

Gao, S., Ling, W., Qiu, Y., Lian, Z., Hartmann, G., Simon, K., 1999. Contrasting geochemical and Sm-Nd isotopic compositions of Archean metasediments from the Kongling high-grade terrain of the Yangtze craton: evidence for cratonic evolution and redistribution of REE

during crustal anatexis. Geochimica Et Cosmochimica Acta 63, 2071-2088.

Gao, W., Zhang, C.H., 2009. Zircon SHRIMP U-Pb ages of the Huangling granite and the tuff beds from Liantuo Formation in the Three Gorges area of Yangtze River, China and its geological significance. Chi. Sci. Bull. 28, 45-50.

Gehrels, G.E., DeCelles, P.G., Ojha, T.P., Upreti, B.N., 2006. Geologic and U-Th-Pb geochronologic evidence for early Paleozoic tectonism in the Kathmandu thrust sheet, central Nepal Himalaya. Geol. Soc. Am. Bull. 118, 185-198.

Geng, Y., Yang, C., Du, L., Wang, X., Ren, L., Zhou, X., 2007. Chronology and tectonic environment of the Tianbaoshan Formation: new evidence from zircon SHRIMP U-Pb age and geochemistry(in Chinese with English abstract). Geological Review 53, 556-563.

Grew, E.S., Carson, C.J., Christy, A.G., Maas, R., Yaxley, G.M., Boger, S.D., Fanning.C.M., 2012. New constraints from U-Pb, Lu-Hf and Sm-Nd isotopic data on the timing of sedimentation and felsic magmatism in the Larsemann Hills, Prydz Bay, East Antarctica. Precambr. Res. 206-207, 87-108.

Guo, J.L., Gao, S., Wu, Y.B., Li, M., Chen, K., Hu, Z.C., Liang, Z.W., Liu, Y.S., Zhou, L., Zong, K.Q., Zhang, W., Chen, H.-H., 2014. 3.45Ga granitic gneisses from the Yangtze Craton, South China: Implications for Early Archean crustal growth. Precambr. Res. 242, 82-95.

Halpin, J.A., Gerakiteys, C.L., Clarke, G.L., Belousova, E.A., Griffin, W.L., 2005. In-situ U-Pb geochronology and Hf isotope analyses of the Rayner Complex, east Antarctica. Contributions to Mineralogy and Petrology 148, 689-706.

Han, K.Y., Wang, L.,Ding, X.Z., Ren, L.D.,Gao, L.Z., Liu, Y.X., Pang, J.F., Xue, J.H.,2016. Provence of sedimentary rocks of Nanhua System in the northern Guangxi Province: Evidence from detrital zircon U-Pb ages. Acta Petrological Sinica 32, 2166-2180.

Hoffman, P.F., 1991. Did the breakout of laurentia turn gondwanaland inside-out? Sci.China Ser. D-Earth Sci. 252, 1409-1412.

Hoffman, P.F., Li, Z.X., 2009. A palaeogeographic context for Neoproterozoic glaciation. Palaeogeography Palaeoclimatology Palaeoecology 277, 158-172.

Hofmann, M., Linnemann, U., Rai, V., Becker, S., Gartner, A., Sagawe, A., 2011. The India and South China cratons at the margin of Rodinia-Synchronous Neoproterozoic magmatism revealed by LA-ICP-MS zircon analyses. Lithos 123, 176-187.

Hu, Z., Liu, Y., Gao, S., Liu, W., Zhang, W., Tong, X., Lin, L., Zong, K., Li, M., Chen, H., Zhou, L., Yang, L., 2012. Improved in situ Hf isotope ratio analysis of zircon using newly designed X skimmer cone and jet sample cone in combination with the addition of nitrogen by laser ablation multiple collector ICP-MS. Journal of Analytical Atomic Spectrometry 27, 1391.

Jackson, S.E., Pearson, N.J., Griffin, W.L., Belousova, E.A., 2004. The application of laser ablation-inductively coupled plasma-mass spectrometry to in situ U-Pb zircon geochronology. Chemical Geology 211, 47-69.

Jacobs, J., Fanning, C.M., Bauer, W., 2003. Timing of Grenville-age vs. Pan-African medium- to high grade metamorphism in western Dronning Maud Land (East Antarctica) and significance for correlations in Rodinia and Gondwana. Precambr. Res. 125, 1-20.

Jiang, G., Sohl. L. E., Christieblick N., 2003. Neoproterozoic stratigraphic comparison of the Lesser Himalaya (India) and Yangtze block (south China): Paleogeographic implications. Geology 31, 917-920.

Ksienzyk, A.K., Jacobs, J., Boger, S.D., Košler, J., Sircombe, K.N., Whitehouse, M.J., 2012. U-Pb ages of metamorphic monazite and detrital zircon from the Northampton Complex: evidence of two orogenic cycles in Western Australia. Precambr. Res. 198-199, 37-50.

Lan, Z.W., Li, X.H., Chu, X., Tang, G., Yang, S., Yang, H., Liu, H., Jiang, T., Wang, T., 2017. SIMS U-Pb zircon ages and Ni-Mo-PGE geochemistry of the lower Cambrian Niutitang Formation in South China: Constraints on Ni-Mo-PGE mineralization and stratigraphic correlations. J. Asi. Earth Sci. 137, 141-162.

Lan, Z.W., Li, X.H., Zhang, Q., Li, Q.L., 2015. Global synchronous initiation of the 2nd episode of Sturtian glaciation: SIMS zircon U-Pb and O isotope evidence from the Jiangkou Group, South China. Precambr. Res. 267, 28-38.

Lan, Z.W., Li, X., Zhu, M., Chen, Z.Q., Zhang, Q., Li, Q., Lu, D., Liu, Y., Tang, G., 2014. A rapid and synchronous initiation of the wide spread Cryogenian glaciations. Precambr. Res. 255, 401-411.

Kinny, P.D., Black, L.P., Sheraton, J.W., 1997. Zircon U-Pb ages and geochemistry of igneous and metamorphic rocks in the northern Prince Charles Mountains, Antarctica. AGSO J. Aust. Geol. Geophys.16, 637-654.

Kinny, P.D., Black, L.P., Sheraton, J.W., 1993. Zircon ages and the distribution of Archaean and

Proterozoic rocks in the Rauer Islands. Antarct. Sci. 5, 193-206

Li, L.M., Sun, M., Wang, Y., Xing, G., Zhao, G., Cai, K., Zhang, Y., 2011. Geochronological and Geochemical study of Palaeoproterozoic gneissic granites and clinopyroxenite xenoliths from NW Fujian, SE China: Implications for the crustal evolution of the Cathaysia Block. J. Asi. Earth Sci. 41, 204-212.

Li, L.M., Lin, S., Xing, G., Jiang, Y., Xia, X., 2018. Geochronology and geochemistry of volcanic rocks from the Jingtan Formation in the eastern Jiangnan orogen, South China: Constraints on petrogenesis and tectonic implications. Precambr. Res. 275, 209-224.

Li, L.M., Lin, S.F., Xing, G.F., Davis, D.W., Jiang, Y., Davis, W., Zhang, Y.J., 2016. Ca. 830Ma back-arc type volcanic rocks in the eastern part of the Jiangnan orogen: Implications for the Neoproterozoic tectonic evolution of South China Block. Precambr. Res. 275, 209-224.

Li, W.X., Li, Z.X., Li, X.H., 2005. Neoproterozoic bimodal magmatism in the Cathaysia Block of South China and its tectonic significance. Precambr. Res. 136, 51-66.

Li, X.H., Li, W.X., Li, Q.L., Wang, X.C., Liu, Y., Yang, Y.H., 2010. Petrogenesis and tectonic significance of the ~850 Ma Gangbian alkaline complex in South China: Evidence from in situ zircon U-Pb dating, Hf-O isotopes and whole-rock geochemistry. Lithos 114, 1-15.

Li, X.H., Li, W.X., Li, Z.X., Lo, C.H., Wang, J., Ye, M.F. Yang, Y.H., 2009. Amalgamation between the Yangtze and Cathaysia Blocks in South China: Constraints from SHRIMP U-Pb zircon ages, geochemistry and Nd-Hf isotopes of the Shuangxiwu volcanic rocks. Precambr. Res. 174,1-2, 117-128.

Li, X.H., 1999. U-Pb zircon ages of granites from the southern margin of the Yangtze Block: timing of Neoproterozoic Jinning: Orogeny in SE China and implications for Rodinia Assembly. Precambr. Res. 97, 43-57.

Li, X.H., Li, Z.X., Ge, W.C., Zhou, H.W., Li, W.X., Liu, Y., Michael, T.D.W., 2003. Neoproterozoic granitoids in South China: crustal melting above a mantle plume at ca. 825 Ma? Precambr. Res. 122, 45-83.

Li, X.H., Li, Z.X., Zhou, H.W., Liu, Y., Kinny, P.D., 2002a. U-Pb zircon geochronology, geochemistry and Nd isotopic study of Neoproterozoic bimodal volcanic rocks in the Kangdian Rift of South China: Implications for the initial rifting of Rodinia. Precambr. Res. 113, 135-154.

Li, X.H., Wang, Y.X., Zhao, Z.H., Chen, D.F., Zhang, h., 1998. SHRIMP U-Pb Zircon geochronology for amphibolite from the precambrain basement in SW Zhejiang and Fujian provinces. Geochimica 27, 327-334.

Li, Z.X., Bogdanova, S.V., Collins, A.S., Davidson, A., De Waele, B., Ernst, R.E., Fitzsimons, I.C.W., Fuck, R.A., Gladkochub, D.P., Jacobs, J., Karlstrom, K.E., Lu, S., Natapov, L.M., Pease, V., Pisarevsky, S.A., Thrane, K., Vernikovsky, V., 2008. Assembly, configuration, and break-up history of Rodinia: A synthesis. Precambr. Res. 160, American Journal of Science179-210.

Li, Z.X., Li, X.H., Zhou, H., Kinny, P.D., 2002b. Grenvillian continental collision in south china: new shrimp u-pb zircon results and implications for the configuration of Rodinia. . Geology 30, 163-166.

Ling, W., Gao, S., Zhang, B.R., Li, H.M., Liu, Y., Cheng, J.P., 2003. Neoproterozoic tectonic evolution of the northwestern Yangtze craton, South China: implications for amalgamation and break-up of the Rodinia Supercontinent. Precambr. Res. 122, 111-140.

Liu, P.J., Li, X.H., Chen, S.M, Lan, Z.W., Yang,B., Shang, X.D., Yin, C.Y., 2015. New SIMS U-Pb zircon age and its constraint on the beginning of the Nantuo glaciation. Science Bulletin 60, 958-963.

Liu, R., Zhou, H., Zhang, L., Zhong, Z., Zeng, W., Xiang, H., Jin, S., Lu, X., Li, C., 2009. Paleoproterozoic reworking of ancient crust in the Cathaysia Block, South China: Evidence from zircon trace elements, U-Pb and Lu-Hf isotopes. Science Bulletin 54, 1543-1554.

Liu, X.C., Wang, W., Zhao, Y., Liu, J., , C., H.,, Cui, Y.C., Song, B., 2016. Early Mesoproterozoic arc magmatism followed by early Neoproterozoic granulite facies metamorphism with a near-isobaric cooling path at Mount Brown, Princess Elizabeth Land, East Antarctica. Precambr. Res. 284, 30-48.

Liu, X.C., Zhao, Y., Chen, H., Song, B., 2017. New zircon U–Pb and Hf–Nd isotopic constraints on the timing of magmatism, sedimentation and metamorphism in the northern Prince Charles Mountains, East Antarctica. Precambr. Res. 299, 15-33.

Liu, X.X., Liu, Z., Zhang, L., Xu,X., 1984. A study of Late Precambrian microfossil algal community from Suining County, Jiangsu Province. Acta Micropalaeontologica Sinica, 1(2):171-182.

Liu, Y., Gao, S., Hu, Z., Gao, C., Zong, K., Wang, D., 2010. Continental and Oceanic Crust Recycling-induced Melt-Peridotite Interactions in the Trans-North China Orogen: U-Pb Dating, Hf Isotopes and Trace Elements in Zircons from Mantle Xenoliths. J. Petrol. 51, 537-571.

Liu, Y., Hu, Z., Gao, S., Günther, D., Xu, J., Gao, C., Chen, H., 2008. In situ analysis of major and trace elements of anhydrous minerals by LA-ICP-MS without applying an internal standard. Chemical Geology 257, 34-43.

Ludwig, K., 2003. A Geochronological Toolkit for Microsoft Excel. Berkeley Geochronology Center, Berkeley, California

McQuarrie, N., Robinson, D., Long, S., Tobgay, T., Grujic, D., Gehrels, G., Ducea, M., 2008. Preliminary stratigraphic and structural architecture of Bhutan: Implications for the along strike architecture of the Himalayan system. Earth. Planet. Sci. Lett. 272, 105-117.

Mikhalsky, E.V., Sheraton, J.W., Labia, A.A., Tingey, R.J., Thost, D.E., Kamenev, E.N., Fedorov, L.V., 2002. Geology of the Prince Charles Mountain, Antarctica. Sci., 14(2), 195-196.

Morrissey, L.J., Hand, M., Kelsey, D.E., 2015. Multi-stage metamorphism in the Rayner-Eastern Ghats Terrane: P-T-t constraints from the northern Prince Charles Mountains, east Antarctica. Precambr. Res. 267, 137-163.

Myrow, P.M., Hughes, N.C., Goodge, J.W., Fanning, C.M., Williams, I.S., Peng, S., Bhargava, O.N., Parcha, S.K., Pogue, K.R., 2010. Extraordinary transport and mixing of sediment across Himalayan central Gondwana during the Cambrian-Ordovician. Geol. Soc. Am. Bull. 122, 1660-1670.

Nesbitt, H., Young, G., 1982. Early Proterozoic climates and plate motions inferred from major element chemistry of lutites. Nature 299, 715–717.

Prave, A.R., Condon, D.J., Hoffmann, K.H., Simon, T., Anthony, E.F., 2016. Duration and nature of the end-Cryogenian (Marinoan) glaciation. Geology 44,8, 631-634.

Phillips, G., Wilson, C.J.L., Campbell, I.H., Allen, C.M., 2006. U-Th-Pb detrital zircon geochronology from the southern Prince Charles Mountains, East Antarctica-Defining the Archaean to Neoproterozoic Ruker Province. Precambr. Res. 148, 292-306.

Pu, J., P., Bowring, S., A., Ramezani, J., Myrow, P., Raub, T.,D., Landing, E., Mills, A., Hodgin, E., Macdonald, F.,A., 2016. Dodging snowballs: Geochronology of the Gaskiers glaciation and

the first appearance of the Ediacaran biota. Geology, 44, 955-958.

Qin, X.F., Pan, Y.M., Li, J., Li, R.S., Zhou, F.S., Hu, G.A., Zhong, F.Y., 2006. Zircon SHRIMP U-Pb geochronology of the Yunkai metamprphoc complex in southeastern Guangxi, China. Sci. China Ser. D-Earth Sci. 25, 553-559.

Rooney, A.D., Strauss, J.V., Brandon, A.D., Macdonald, F.A., 2015. A Cryogenian chronology: Two long-lasting synchronous Neoproterozoic glaciations. Geology 43, 459-462.

Sarjeant, W.A.S., Stancliffe, R.P.W., 1994. The Micrhystridium and Veryhachium Complexes (Acritarcha: Acanthomorphitae and Polygonomorphitae): A Taxonomic Reconsideration. Micropaleontology. 40, 1-77.

Shu, L.S., Faure, M., Yu, J.H., Jahn, B.M., 2011. Geochronological and geochemical features of the Cathaysia block (South China): New evidence for the Neoproterozoic breakup of Rodinia. Precambr. Res. 187, 263-276.

Shu, L.S., Deng, P., Yu, J.H., Wang, Y.B., Jiang, S.Y., 2008a. The age and tectonic environment of the rhyolitic rocks on the western side of Wuyi Mountain, South China. Sci. China Ser. D-Earth Sci. 51, 1053-1063.

Shu, L.S., Jahn, B.M., Charvet, J., Santosh, M., Wang, B., Xu, X.S., Jiang, S.Y., 2014. Early Paleozoic depositional environment and intraplate tectono-magmatism in the Cathaysia Block (South China): Evidence from stratigraphic, structural, geochemical and geochronological investigations. Am. J. Sci. 314, 154-186.

Shu, L.S., Yu, J.H., Jia, D., Wang, B., Shen, W.Z., Zhang, Y.Q., 2008b. Early Paleozoic orogenic belt in the eastern segment of South China. Sci. China Ser. D-Earth Sci. 27, 1581-1593.

Shukla M, Babu R, Mathur V K, D, S., 2005. Additional Terminal Proterozoic organic-walled microfossils from the Infra-Krol Formation, Nainital Syncline, Lesser Himalaya, Uttaranchal. Journal of the Geological Society of India 65, 197-210.

Spencer, C.J., Harris, R.A., Dorais, M.J., 2012. Depositional provenance of the Himalayan metamorphic core of Garhwal region, India: Constrained by U-Pb and Hf isotopes in zircons. Gondwana Res. 22, 26-35.

Tewari, V.C., 2001. Discovery and sedimentology of microstromatolites from Menga Limestone (NeoproterozoicN endian), Upper Subansiri district, Arunachal Pradesh, NE Himalaya, India. Current Science 80, 1440-1444.

Thomson, M.R.A.,1977. An annotated bibliography of the paleontology of Lesser Antarctica and the Scotia Ridge. New Zealand Journal of Geology & Geophysics. 20(5):865-904.

Tsunogae, T., Yang, Q.-Y., Santosh, M., 2015. Early Neoproterozoic arc magmatism in the Lützow-Holm Complex, East Antarctica: Petrology, geochemistry, zircon U-Pb geochronology and Lu-Hf isotopes and tectonic implications. Precambr. Res. 266, 467-489.

Veevers, J.J., Saeed, A., 2009. Permian-Jurassic Mahanadi and Pranhita-Godavari Rifts of Gondwana India: Provenance from regional paleoslope and U-Pb/Hf analysis of detrital zircons. Gondwana Res. 16, 633-654.

Veevers, J.J., Saeed, A., 2011. Age and composition of Antarctic bedrock reflected by detrital zircons, erratics, and recycled microfossils in the Prydz Bay-Wilkes Land-Ross Sea-Marie Byrd Land sector (70°-240°E). Gondwana Res. 20, 710-738.

Veevers, J.J., Saeed, A., Belousova, E.A., Griffin, W.L., 2005. U-Pb ages and source composition by Hf-isotope and trace-element analysis of detrital zircons in Permian sandstone and modern sand from southwestern Australia and a review of the paleogeographical and denudational history of the Yilgarn Craton. Earth-Sci Rev. 68, 245-279.

Wan, Y., Liu, D., Xu, M., Zhuang, J., Song, B., Shi, Y., Du, L., 2007. SHRIMP U-Pb zircon geochronology and geochemistry of metavolcanic and metasedimentary rocks in Northwestern Fujian, Cathaysia block, China: Tectonic implications and the need to redefine lithostratigraphic units. Gondwana Res. 12, 166-183.

Wang, J., Li, X.H., Duan, T.Z., Liu, D.Y., Song, B., Li, Z.X., Gao, Y.H., 2003. Zircon SHRIMPU-PbdatingfortheCangshuipuvolcanicrocksanditsimplicationsforthelowerboundarya geoftheNanhuastratainSouthChina. Science Bulletin 48, 1663-1669.

Wang, J.Q., Shu, L.S., Santosh, M.,2017a. U-Pb and Lu-Hf isotopes of detrital zircon grains from Neoproterozoic sedimentary rocks in the central Jiangnan Orogen, South China: Implications for Precambrian crustal evolution. Precambr. Res. 294: 175-188.

Wang, Z., Zhou, B., Guo, Y., Yang, B., Liao, Z., Wang, S., 2012a. Geochemistry and zircon U-Pb dating of Tangtang granite in the western margin of the Yangtze Platform. Acta Petrologica et Mineralogica 31, 652 – 662 (in Chinese with English abstract).

Wang, W., Zeng, M.F., Zhou, M.F., Zhao, J.H., Zheng, J.P., Lan, Z.F., 2018. Age, provenance and tectonic setting of Neoproterozoic to early Paleozoic sequences in southeastern South China

Block: Constraints on its linkage to western Australia-East Antarctica. Precambr. Res. 309: 290-308.

Wang, W., Zhou, M.F., Yan, D.P., Li, L., Malpa, J., 2013a. Detrital zircon record of Neoproterozoic active-margin sedimentation in the eastern Jiangnan Orogen, South China. Precambr. Res. 235, 1-19.

Wang, X.L., Zhou, J.C., Griffin, W.L., Wang, R.C., Qiu, J.S., O'Reilly, S.Y., Xu, X., Liu, X.M., Zhang, G.L., 2007. Detrital zircon geochronology of Precambrian basement sequences in the Jiangnan orogen: Dating the assembly of the Yangtze and Cathaysia Blocks. Precambr. Res. 159, 117-131.

Wang, X.L., Zhou, J.C., Qiu, J.S., Zhang, W.L., Liu, X.M., Zhang, G.L., 2006. LA-ICP-MS U-Pb zircon geochronology of the Neoproterozoic igneous rocks from Northern Guangxi, South China: Implications for tectonic evolution. Precambr. Res. 145, 111-130.

Wang, X., Chen, J., Luo, D., 2008a. Study on Petrogenesis of Zircons from the Danzhu Granodiorote and Its Geological Implications. Geological Review 54, 387-398.

Wang, X.C., Li, X.H., Li, W.X., Li, Z.X., Liu, Y., Yang, Y.H., Liang, X.R., Tu, X.L., 2008b. The Bikou basalts in the northwestern Yangtze block, South China: Remnants of 820-810 Ma continental flood basalts? Geol. Soc. Am. Bull. 120, 1478-1492.

Wang, X.L., Zhou, J.C., Griffin, W.L., Zhao, G.C., Yu, J.H., Qiu, J.S., Zhang, Y.J., Xing, G.F., 2014a. Geochemical zonation across a Neoproterozoic orogenic belt: Isotopic evidence from granitoids and metasedimentary rocks of the Jiangnan orogen, China. Precambr. Res. 242, 154-171.

Wang, Y.J., Wu, C., Zhang, A., Fan, W., Zhang, Y., Zhang, Y., Peng, T., Yin, C., 2012b. Kwangsian and Indosinian reworking of the eastern South China Block: Constraints on zircon U-Pb geochronology and metamorphism of amphibolites and granulites. Lithos 150, 227-242.

Wang, Y.J., Zhang, A., Cawood, P.A., Fan, W., Xu, J., Zhang, G., Zhang, Y., 2013b. Geochronological, geochemical and Nd-Hf-Os isotopic fingerprinting of an early Neoproterozoic arc-back-arc system in South China and its accretionary assembly along the margin of Rodinia. Precambr. Res. 231, 343-371.

Wang, Y.J., Zhang, A., Fan, W., Zhao, G., Zhang, G., Zhang, Y., Zhang, F., Li, S., 2011. Kwangsian crustal anatexis within the eastern South China Block: Geochemical, zircon U-Pb

geochronological and Hf isotopic fingerprints from the gneissoid granites of Wugong and Wuyi-Yunkai Domains. Lithos 127, 239-260.

Wang, Y.J., Zhang, F.F., Fan, W.M., Zhang, G.W., Chen, S.Y., Cawood, P.A., Zhang, A.M., 2010. Tectonic setting of the South China Block in the early Paleozoic: Resolving intracontinental and ocean closure models from detrital zircon U-Pb geochronology. Tectonics 29, 1-16.

Wang, Y.J., Zhang, Y.Z., Fan, W.M., Geng, H.Y., Zou, H.P., Bi, X.W., 2014b. Early Neoproterozoic accretionary assemblage in the Cathaysia Block: Geochronological, Lu-Hf isotopic and geochemical evidence from granitoid gneisses. Precambr. Res. 249, 144-161.

Wang, Z.J., Jiang, X.S., Du, Q.D., Deng, Q., Yang, F., Wu, H., Zhou, X.L., 2013c. Depositional Transformation from Banxi Period to Nanhua Glacial Period in Southeast Margin of Yangtze Block and its Implications to Stratigraphic Correlation. Acta Sedimentologica Sinica 31, 385-395.

Wang, Z., Wang J., Suess, E., Wang, G., Z., Xiao, S.H., 2017. Silicified glendonites in the Ediacaran Doushantuo Formation (South China) and their potential paleoclimatic implications. Geology 45(2), 115-118

Xiang, H., Zhang, L., Zhou, H.W., Zhong, Z.Q., Zeng, W., Liu, R., Ji, S., 2008. Metamorphic zircon SHRIMP U-Pb, Hf isotope geochronology of the basic-ultrabasic metamprphoc basement in southwestern Zhejiang province. Sci.China Ser. D-Earth Sci. 38, 401-413.

Xin, Y., Li, J., Dong, S., Zhang, Y., Wang, W., Sun, H., 2017. Neoproterozoic post-collisional extension of the central Jiangnan Orogen: Geochemical, geochronological, and Lu-Hf isotopic constraints from the ca. 820-800 Ma magmatic rocks. Precambr. Res. 294, 91-110.

Xing, G.F., Wang, X.L., Wan, Y., Chen, Z.H., Jiang, Y., Kitajima, K., Ushikubo, T., Gopon, P., 2014. Diversity in early crustal evolution: 4100 Ma zircons in the Cathaysia Block of southern China. Sci Rep. 4, 5143.

Xu, X.B., Zhang, Y.Q., Shu, L.S., Jia, D., Wang, R.R., Xu, H.Z., 2010. Precambian Geochronology and Stratigraphy in the Wuyishan Area, South Chian. Journal of Stratigraphy 34, 254-267.

Xu, Y.J., Cawood, P.A., Du, Y.S., 2016. Intraplate orogenesis in response to Gondwana assembly: Kwangsian Orogeny, South China. Am.J.Sci. 316, 329-362.

Xu, Y.J., Cawood, P.A., Du, Y.S., Hu, L.S., Yu, W.C., Zhu, Y.H., Li, W.C., 2013. Linking south

China to northern Australia and India on the margin of Gondwana: Constraints from detrital zircon U-Pb and Hf isotopes in Cambrian strata. Tectonics 32, 1547-1558.

Xu, Y.J., Cawood, P.A., Du, Y.S., Huang, H.W., Wang, X.Y., 2014a. Early Paleozoic orogenesis along Gondwana's northern margin constrained by provenance data from South China. Tectonophysics 636, 40-51.

Xu, Y.J., Cawood, P.A., Du, Y.S., Zhong, Z.Q., Hughes, N.C., 2014b. Terminal suturing of Gondwana along the southern margin of South China Craton: Evidence from detrital zircon U-Pb ages and Hf isotopes in ambrian and Ordovician strata, Hainan Island. Tectonics, 33, 2490-2504，doi:10.1002/2014TC003748

Xue, H., Ma, F., Song, Y.Q., Xie, Y.P., 2010. Geochronology and geochemisty of the Neoproterozoic granitoid association from eastern segment of the Jiangnan orogen, China: Constraints on the timing and process of amalgamation between the Yangtze and Cathaysia blocks. Acta Petrologica Sinica 26, 3215-3244.

Yao, J.L., Shu, L.S., Santosh, M., Li, J.Y., 2013. Geochronology and Hf isotope of detrital zircons from Precambrian sequences in the eastern Jiangnan Orogen: Constraining the assembly of Yangtze and Cathaysia Blocks in South China. J. Asi. Earth Sci. 74, 225-243.

Yao, J.L., Shu, L.S., Santosh, M., Li, J.Y., 2015. Neoproterozoic arc-related andesite and orogeny-related unconformity in the eastern Jiangnan orogenic belt: Constraints on the assembly of the Yangtze and Cathaysia blocks in South China. Precambr. Res. 262, 84-100.

Yao, W.H., Li, Z.X., Li, W.X., Li, X.H., Yang, J.H., 2014. From Rodinia to Gondwanaland: A tale of detrital zircon provenance analyses from the southern Nanhua Basin, South China. Am.J.Sci. 314, 278-313.

Ye, M.F., Li, X.H., Li, W.X., Liu, Y., Li, Z.X., 2007. SHRIMP zircon U-Pb geochronological and whole-rock geochemical evidence for an early Neoproterozoic Sibaoan magmatic arc along the southeastern margin of the Yangtze Block. Gondwana Res. 12, 144-156.

Yin, C.Y., Tang, F., Liu, Y.Q., Gao, L.Z., Yang, Z.Q., Wang, Z.Q., Liu, P.J., Xing, Y.S., Song, B., 2005. New U-Pb zircon ages from the Ediacaran (Sinian) System in the Yangtze Gorges: Constraint on the age of Miaohe biota and Marinoan glaciation. Chin. Sci. Bull. 24(5), 393-400.

Yu, J.H., O'Reilly, S.Y., Zhou, M.-F., Griffin, W.L., Wang, L., 2012. U-Pb geochronology and

Hf-Nd isotopic geochemistry of the Badu Complex, Southeastern China: Implications for the Precambrian crustal evolution and paleogeography of the Cathaysia Block. Precambr. Res. 222-223, 424-449.

Yu, J.H., O'Reilly, Y.S., Wang, L., Griffin, W.L., Jiang, S., Wang, R., Xu, X., 2007. Finding of ancient materials in Cathaysia and implication for the formation of Precambrian crust. Chin. Sci. Bull. 52, 13-22.

Yu, J.H., O'Reilly, S.Y., Wang, L.J., Griffin, W.L., Zhang, M., Wang, R.C., Jiang, S.Y., Shu, L.S., 2008. Where was South China in the Rodinia supercontinent? Precambr. Res. 164, 1-15.

Yu, J.H., Wang, L.J., O'Reilly, S.Y., Griffin, W.L., Zhang, M., Li, C.Z., Shu, L.S., 2009. A Paleoproterozoic orogeny recorded in a long-lived cratonic remnant (Wuyishan terrane), eastern Cathaysia Block, China. Precambr. Res. 174, 347-363.

Yu, J.H., Zhou, X.M., Reilly, Y.S.O., ZHAO, L., Griffin, W.L., Wang, R.C., Wang, L.J., Chen, X.M., 2005. Formation history and protolith characteristics of granulite facies metamorphic rock in Central Cathaysia deduced from U-Pb and Lu-Hf isotopic studies of single zircon grains. Chin. Sci. Bull. 50, 2080.

Zhang, A., Wang, Y., Fan, W., Zhang, Y., Yang, J., 2012a. Earliest Neoproterozoic (ca. 1.0Ga) arc-back-arc basin nature along the northern Yunkai Domain of the Cathaysia Block: Geochronological and geochemical evidence from the metabasite. Precambr. Res. 220-221, 217-233.

Zhang, F.F., Wang, Y.J., Fan, W.M., Zhang, A.M., Zhang, Y.Z., 2011. ircon U-Pb geochronology and Hf isotopes of the Neoproterozoic granites in the central of Jiangnan Uplift. Geotectonica Et Metallogenia 35, 73-94.

Zhang, K.B., CHEN, J.L., Lin, H.C., Huang, C.Q., Luo, Z.X., 2005. Lithostratigraphic division and correlation of the Nanhuaan-Sinian Periods in southwestern Fujian. Chinese Geology 32, 363-369.

Zhang, S.B., Zheng, Y.F., Wu, Y.B., Zhao, Z.F., Gao, S., Wu, F.Y., 2006. Zircon U-Pb age and Hf isotope evidence for 3.8 Ga crustal remnant and episodic reworking of Archean crust in South China. Earth. Planet. Sci. Lett. 252, 56-71.

Zhang, S., Jiang, G., Han, Y., 2008. The age of the Nantuo Formation and Nantuo glaciation in South China. Terra Nova 20, 289-294.

Zhang, Y., Wang, Y., Fan, W., Zhang, A., Ma, L., 2012b. Geochronological and geochemical constraints on the metasomatised source for the Neoproterozoic ~825Ma) high-mg volcanic rocks from the Cangshuipu area (Hunan Province) along the Jiangnan domain and their tectonic implications. Precambr. Res. 220-221, 139-157.

Zhang, Z.L., Yuan, H.H., Nan, Y., 1998. Whole-grain zircon evaporation for age of Luoyu Formation, Yunkai Group. J. Mineral. Petro. 18, 85-90.

Zhao, G.C., Cawood, P.A., 2012. Precambrian geology of China. Precambr. Res. 222-223, 13-54.

Zhao, Y. Y., Zheng, Y. F., 2011. Record and time of Neoproterozoic glaciations on Earth. Acta. Petrol. Sin. 27, 545-565.

Zheng, J.P., Griffin, W.L., O'Reilly, S.Y., Zhang, M., Pearson, N.J., Pan, Y.M., 2006. Widespread Archean basement beneath the Yangtze craton. Geology 34, 417.

Zheng, Y.F., Wu, R.X., Wu, Y.B., Zhang, S.B., Yuan, H., Wu, F.Y., 2008. Rift melting of juvenile arc-derived crust: Geochemical evidence from Neoproterozoic volcanic and granitic rocks in the Jiangnan Orogen, South China. Precambr. Res. 163, 351-383.

Zhou, C.M., Tucker, R., Xiao, S., Peng, Z., Yuan, X., Chen, Z., 2004. New constraints on the ages of Neoproterozoic glaciations in south China. Geology 32, 437.

Zhou, J.C., Wang, X.L., Qiu, J.S., 2009. Geochronology of Neoproterozoic mafic rocks and sandstones from northeastern Guizhou, South China: Coeval arc magmatism and sedimentation. Precambr. Res. 170, 27-42.

Zhu, D.C., Zhao, Z.D., Niu, Y., Dilek, Y., Mo, X.X., 2011. Lhasa terrane in southern Tibet came from Australia. Geology 39, 727-730.

Figure Captions

Fig. 1. (a) Tectonic outline of east Eurasia (modified from Cawood et al., 2018), and (b) simplified geological map of the South China Craton showing the main tectono-stratigraphic units (modified from Xu et al., 2013 and Cawood et al., 2018). Sources of age data for Neoproterozoic volcanic rocks given in reference list.

Fig. 2. Representative lithologies and correlations of Cryogenian to Ediacaran strata in selected regions from the South China Craton (data from BGMRGP, 1987; 1988; 1985; BGMRFP, 1985)

Fig. 3. Simplified geological map and sample locations in the (a) Changting area, southern Wuyi region, (b) Nanxiong area, northern Nanling region, (c) Sanjiang area, western Jiangnan orogen.

Fig. 4. CL images of representative zircons showing main types of internal structures from 4 sample regions. (a) Changting area, (b) Nanxiong area, (c) Sanjiang area, (d) Jinping area. Red circles show location of U-Pb analysis spots, and white circles denote Lu-Hf analysis spots.

Fig. 5. U-Pb concordia diagrams of detrital zircon analyses.

Fig. 6. Relative probability density diagrams of ages within 10% of concordia for the analyzed samples.

Fig. 7. Summary of $\varepsilon_{Hf}(t)$ data for detrital zircon grains from the studied sedimentary rocks within 10% of concordia for the analyzed samples. Comparative data from the Tethyan Himalaya -India (Spencer et al., 2012; Zhu et al., 2011), Australia (Veevers et al., 2005), Antarctica (Grew et al., 2012), Rayner Complex /E.Ghats (Halpin et al., 2005; Veevers and Saeed, 2009, 2011), and Jiangnan orogen (Cui et al., 2017; Li et al., 2018; Wang et al., 2008c; Yao et al., 2013; Yin et al., 2013).

Fig. 8. Stratigraphic column and chemical index of alteration (CIA), chemical index of weathering (CIW) from the Louziba to Huanglian formations and from the Xixi Formation in Changting area, southern Wuyi region.

Fig. 9. Stratigraphic correlation chart for late Neoproterozoic to early Paleozoic rock units overlying the Jiangnan Orogen and Cathaysia Block of the South China Craton. Radiometric ages are from Condon et al. (2005), Gao and Zhang (2009), Lan et al. (2017), Lan et al. (2015), Lan et al. (2014), Regional Survey of Fujian province (2017), Wang et al. (2013c), Yu et al. (2005), Zhang et al. (2008), and Zhou et al. (2004).

Fig. 10. Compilation of detrital zircon age distribution of (a) Cryogenian samples in the Yangtze Block (this study), (b) Cryogenian and Ediacaran samples in the

Cathaysia Block (this study), (c) Neoproterozoic samples in the Greater Himalaya (Gehrels et al., 2006; McQuarrie et al., 2008), (d) Neoproterozoic samples in India (Chattopadhyay et al., 2015; Dharma Rao et al., 2013), (e) Neoproterozoic samples in East Antarctica (Boger et al., 2000; Jacobs et al., 2003; Tsunogae et al., 2015), and (f) Neoproterozoic samples in Western Australia (Ksienzyk et al., 2012). Important age peaks are shown in color bands. n = total number of analyses. All data based on analyses within 10% of concordia. Ages greater than 1000 Ma are calculated using $^{207}Pb/^{206}Pb$ ratios, and ages less than 1000 Ma are calculated from $^{206}Pb/^{238}U$ ratios.

Fig. 11. Compilation of detrital zircon age distribution of (a) Cryogenian and lower Ediacaran samples in the Cathaysia Block (this study), (b) and upper Ediacaran samples in the Cathaysia Block (this study).

Fig. 12 Paleoposition of the SCC relative to Cryogenian to Ediacaran supercontinents (modified after Hoffman et al., 1991; Phillips et al., 2006; Xu et al., 2013). The red star represents the location of the studied sequences in the Cathaysia Block.

Highlights

(1) A late Cryogenian and an Ediacaran climate cooling events recognized within siliciclastic strata overlying the Cathaysia Block, South China, and likely coincide with the global Marinoan and Gaskiers glaciations.

(2) Cryogenian siliciclastic rocks overlying the Jiangnan Orogen were derived from local sources within South China.

(3) Late Crogenian and Ediacaran siliciclastic rocks derived from sources external to the craton.

(4) South China Craton linked to northern India since the Cryogenian.

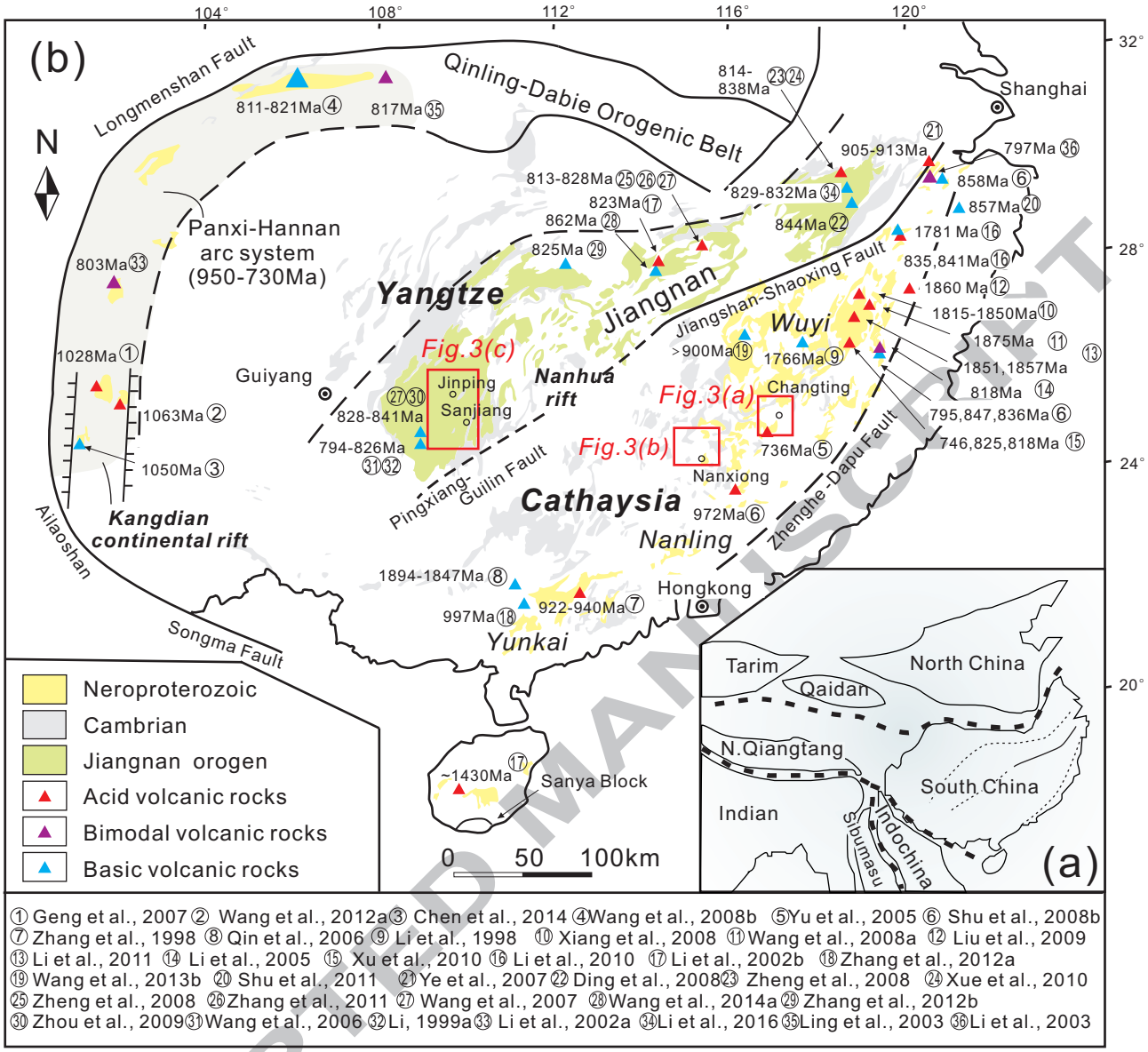

① Geng et al., 2007 ② Wang et al., 2012a ③ Chen et al., 2014 ④Wang et al., 2008b ⑤Yu et al., 2005 ⑥ Shu et al., 2008b
⑦ Zhang et al., 1998 ⑧ Qin et al., 2006 ⑨ Li et al., 1998 ⑩ Xiang et al., 2008 ⑪Wang et al., 2008a ⑫ Liu et al., 2009
⑬ Li et al., 2011 ⑭ Li et al., 2005 ⑮ Xu et al., 2010 ⑯ Li et al., 2010 ⑰ Li et al., 2002b ⑱Zhang et al., 2012a
⑲ Wang et al., 2013b ⑳ Shu et al., 2011 ㉑ Ye et al., 2007 ㉒ Ding et al., 2008 ㉓ Zheng et al., 2008 ㉔ Xue et al., 2010
㉕ Zheng et al., 2008 ㉖Zhang et al., 2011 ㉗ Wang et al., 2007 ㉘Wang et al., 2014a ㉙ Zhang et al., 2012b
㉚ Zhou et al., 2009 ㉛Wang et al., 2006 ㉜Li, 1999a ㉝ Li et al., 2002a ㉞Li et al., 2016 ㉟Ling et al., 2003 ㊱Li et al., 2003

Fig. 1

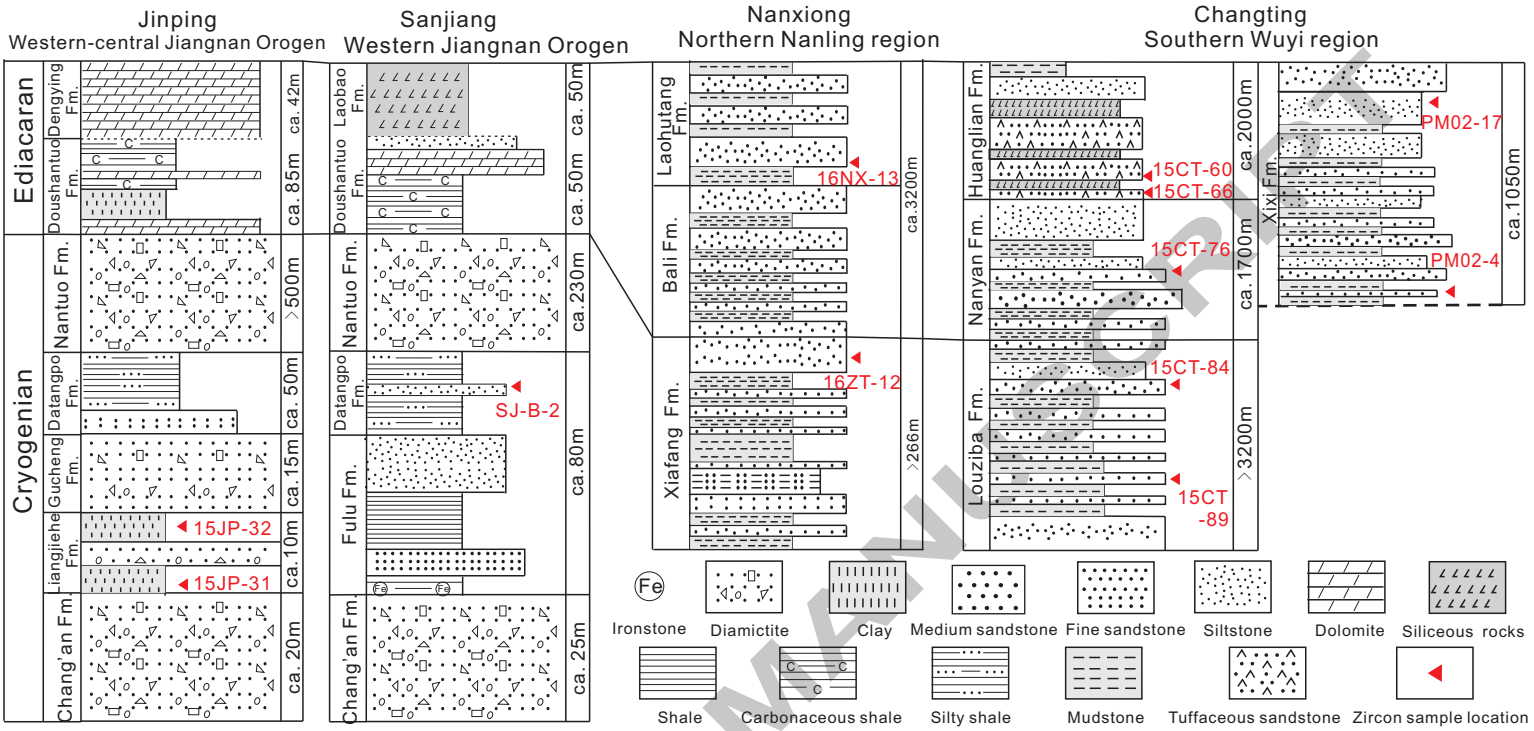

Fig. 2

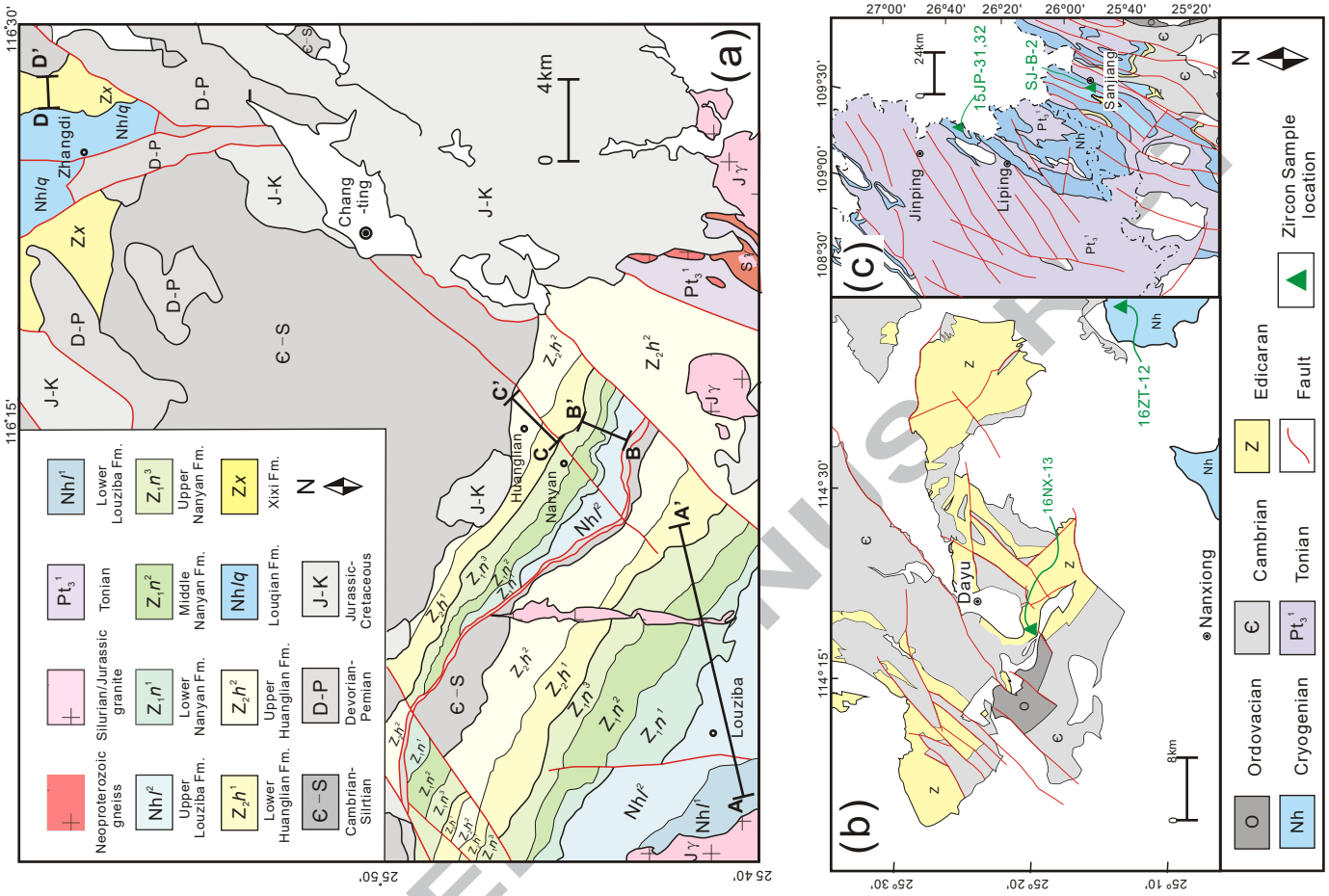

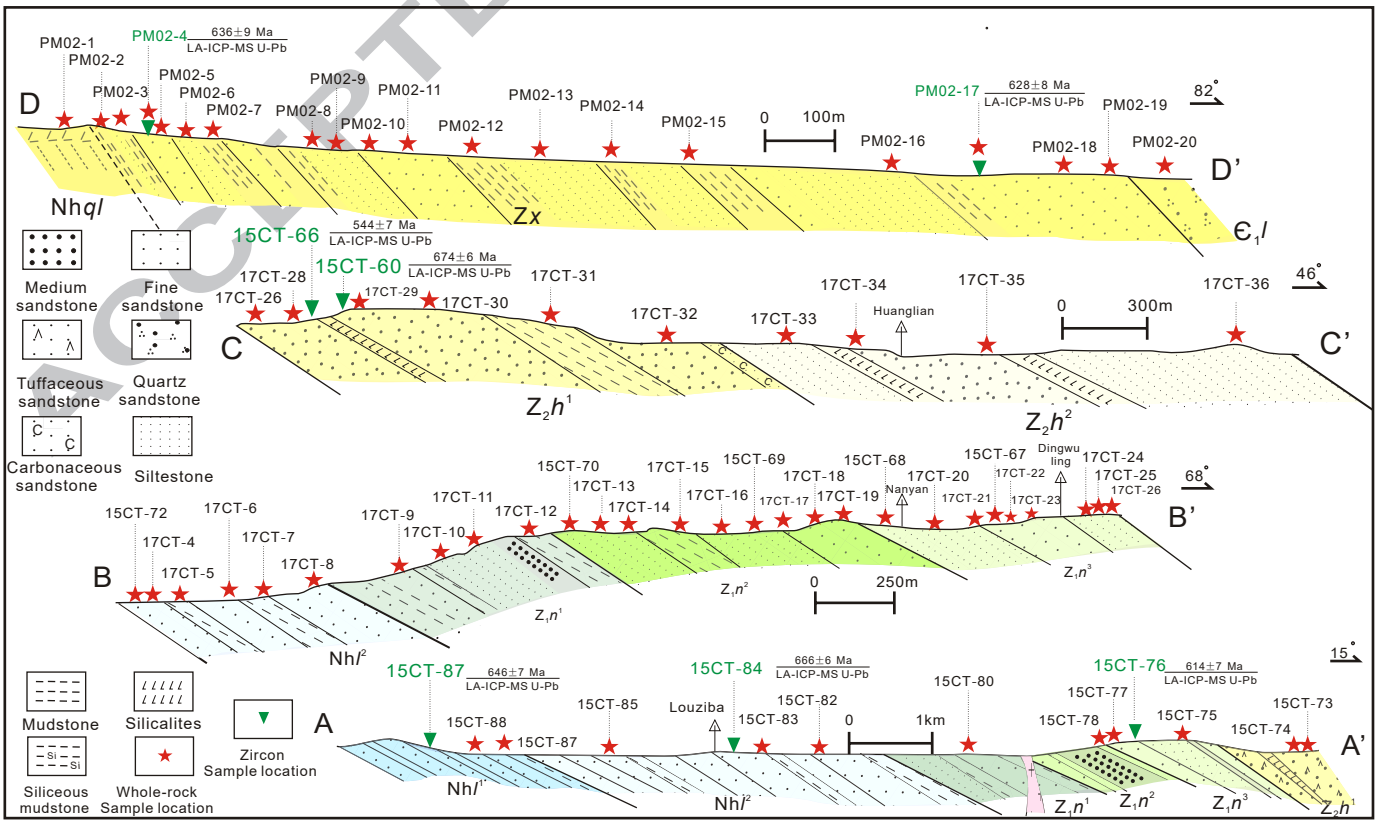

Fig.3

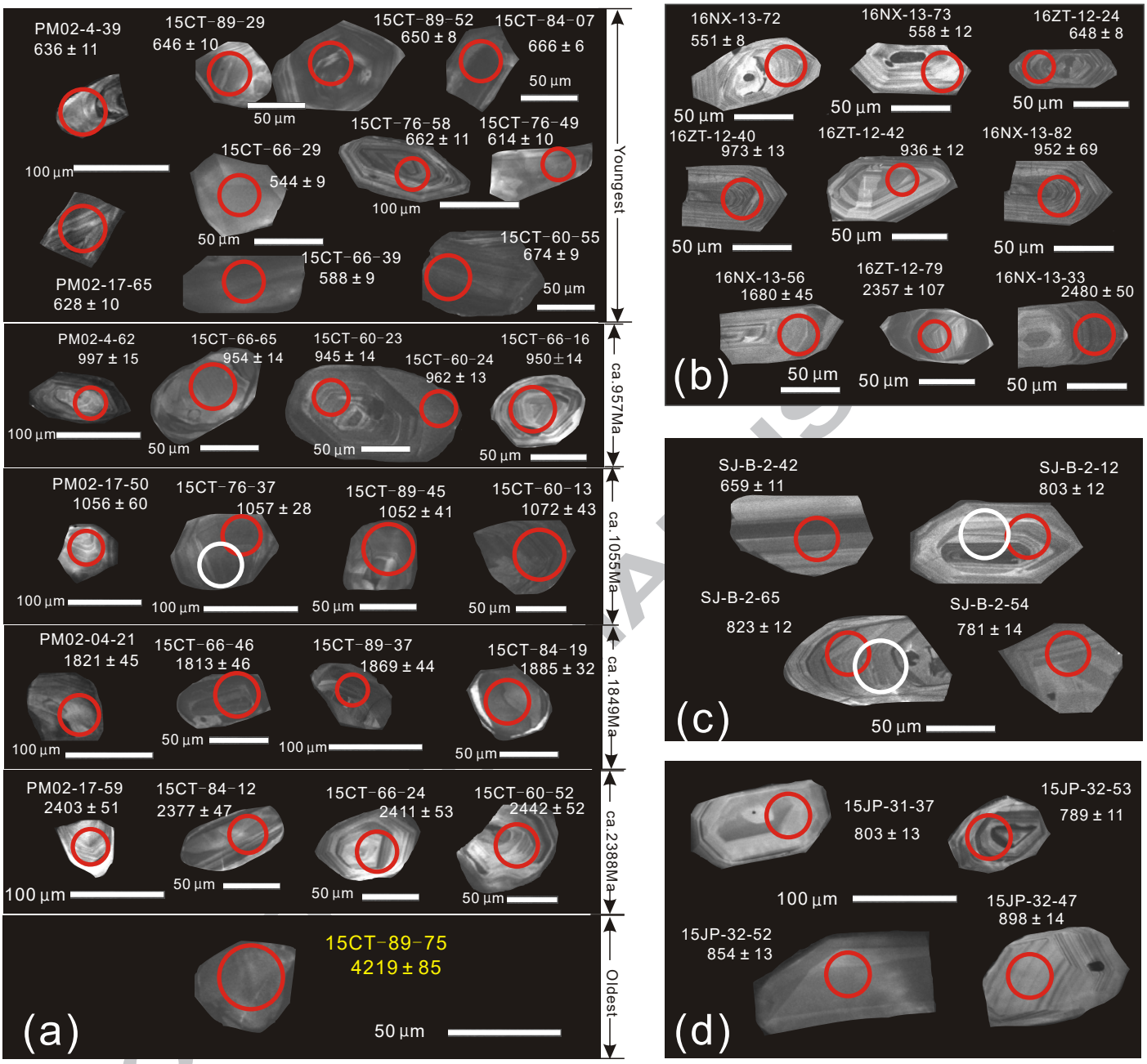

Fig. 4

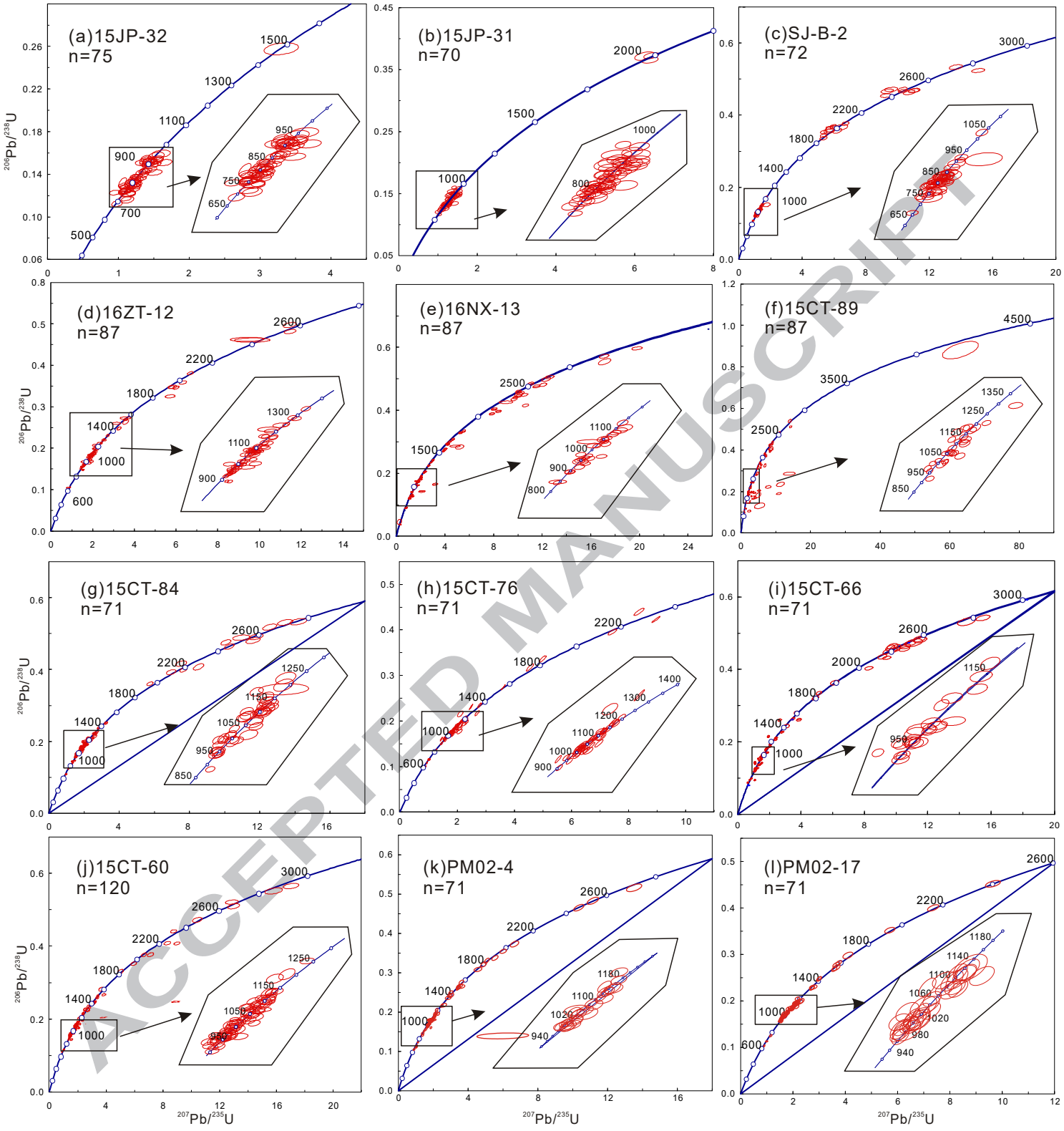

Fig. 5

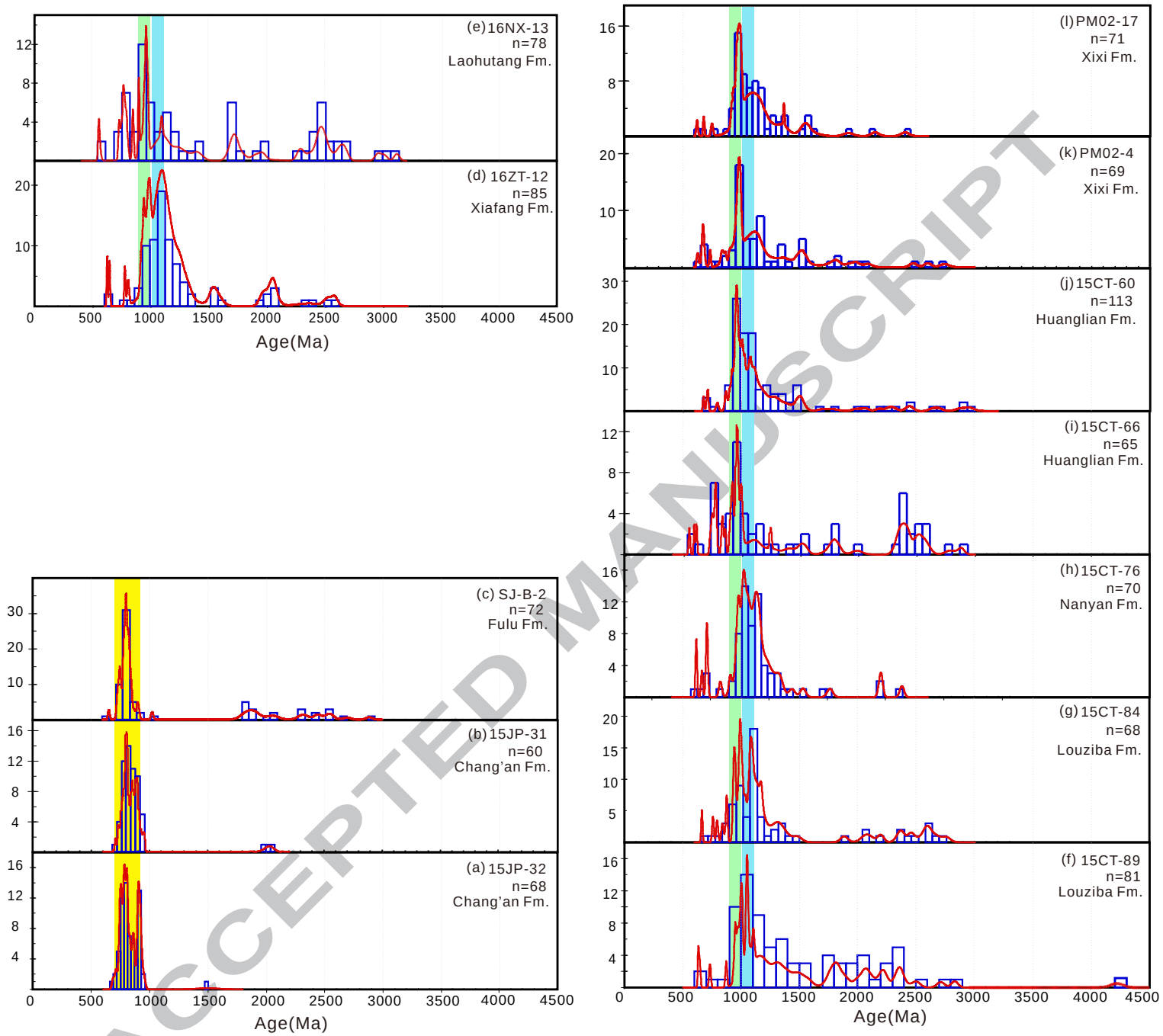

Fig. 6

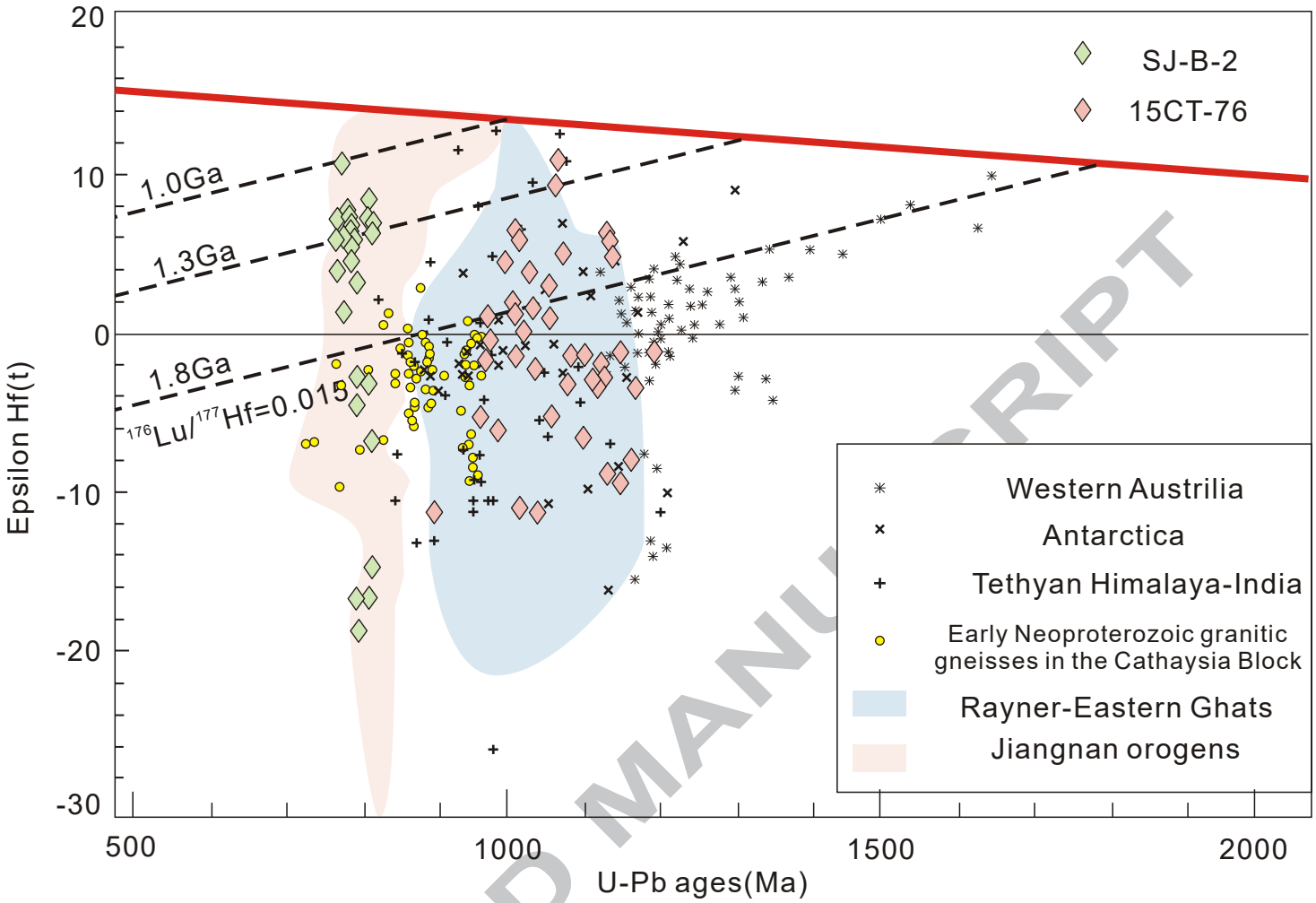

Fig. 7

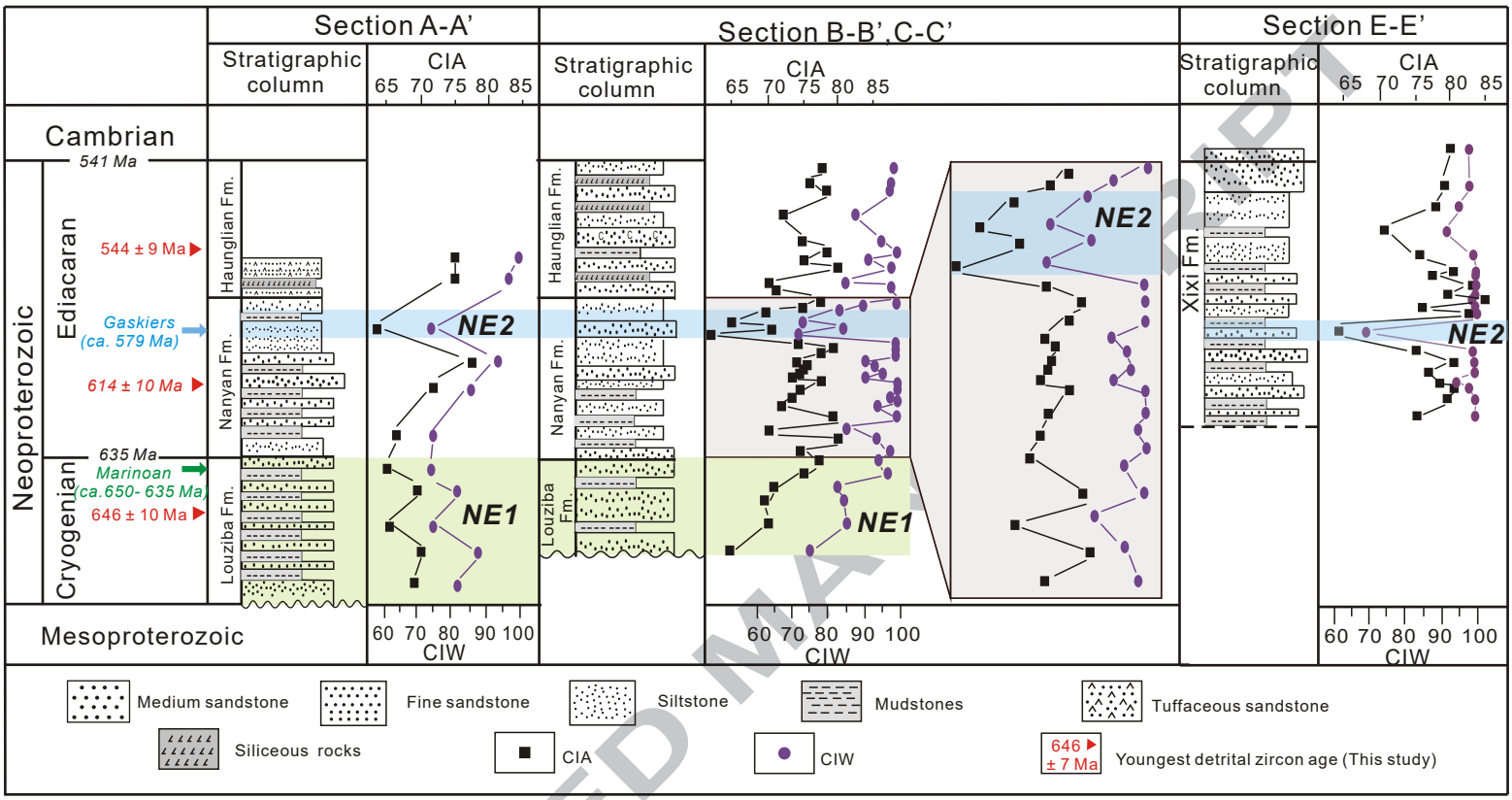

Fig. 8

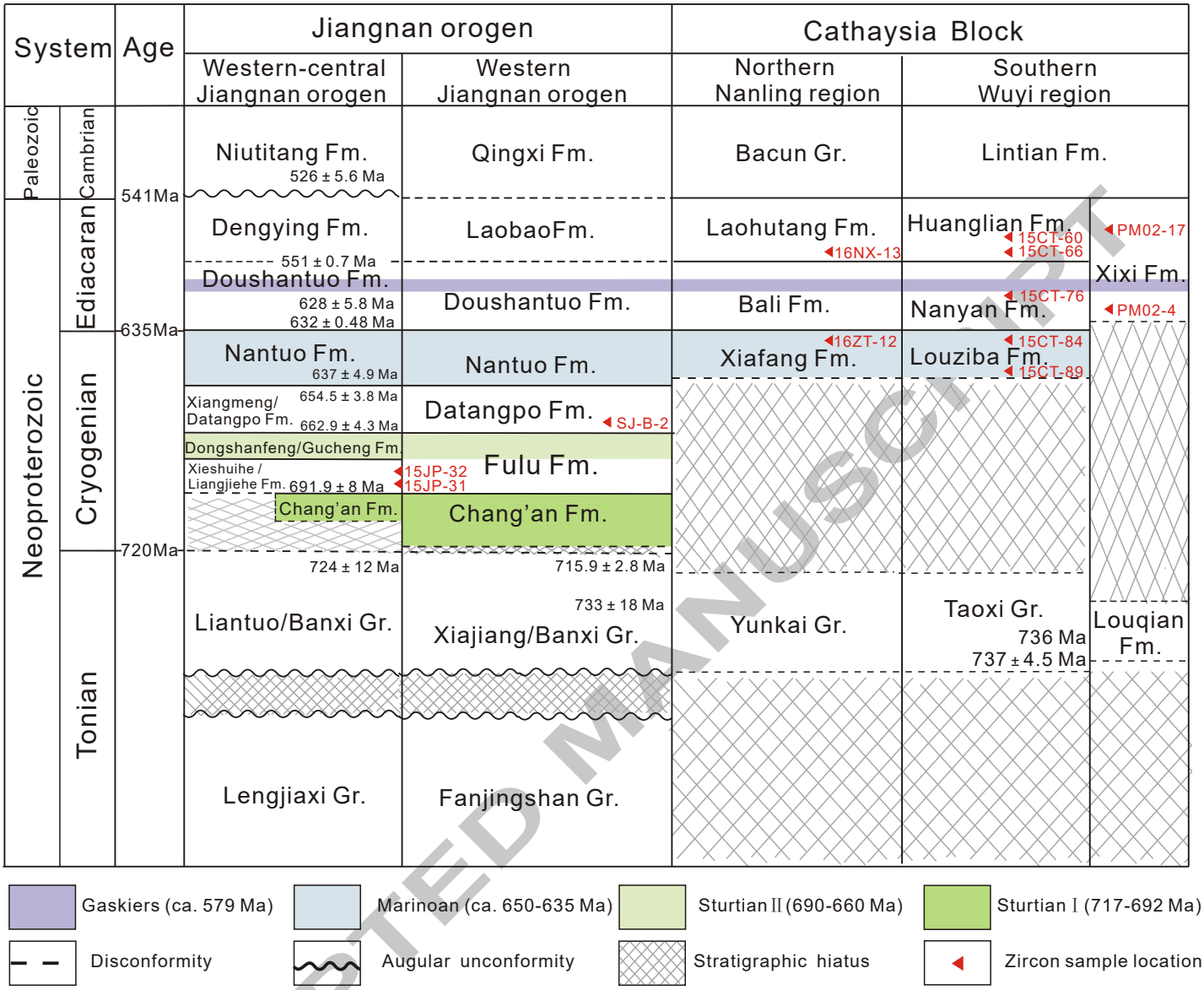

Fig. 9

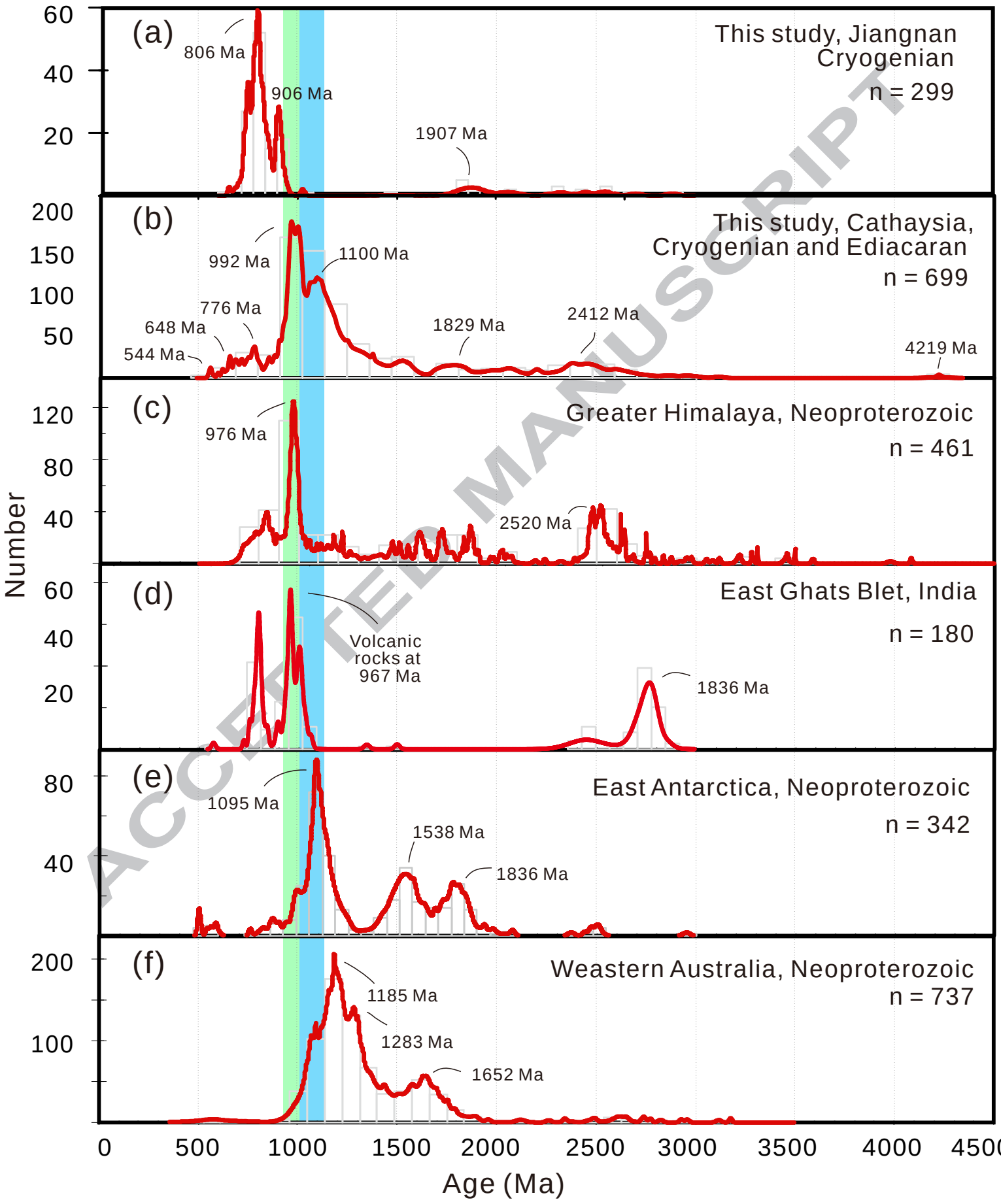

Fig. 10

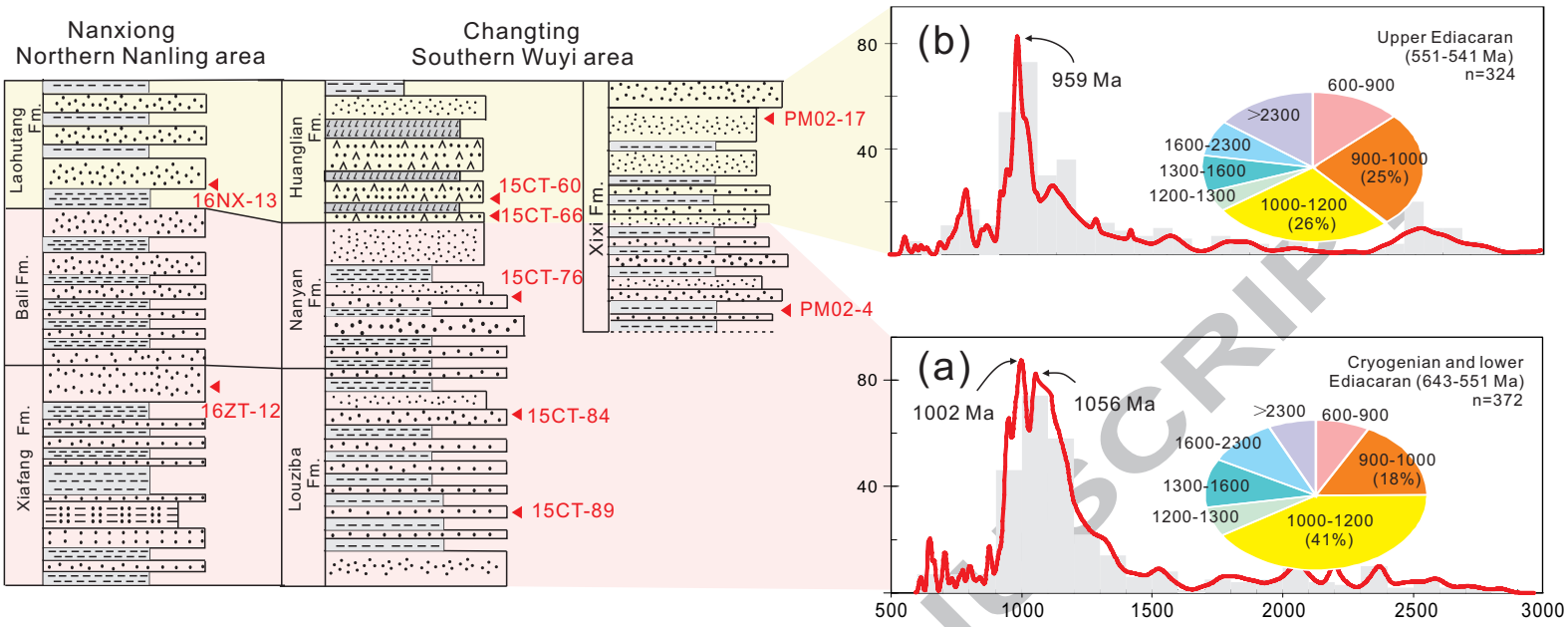

Fig. 11

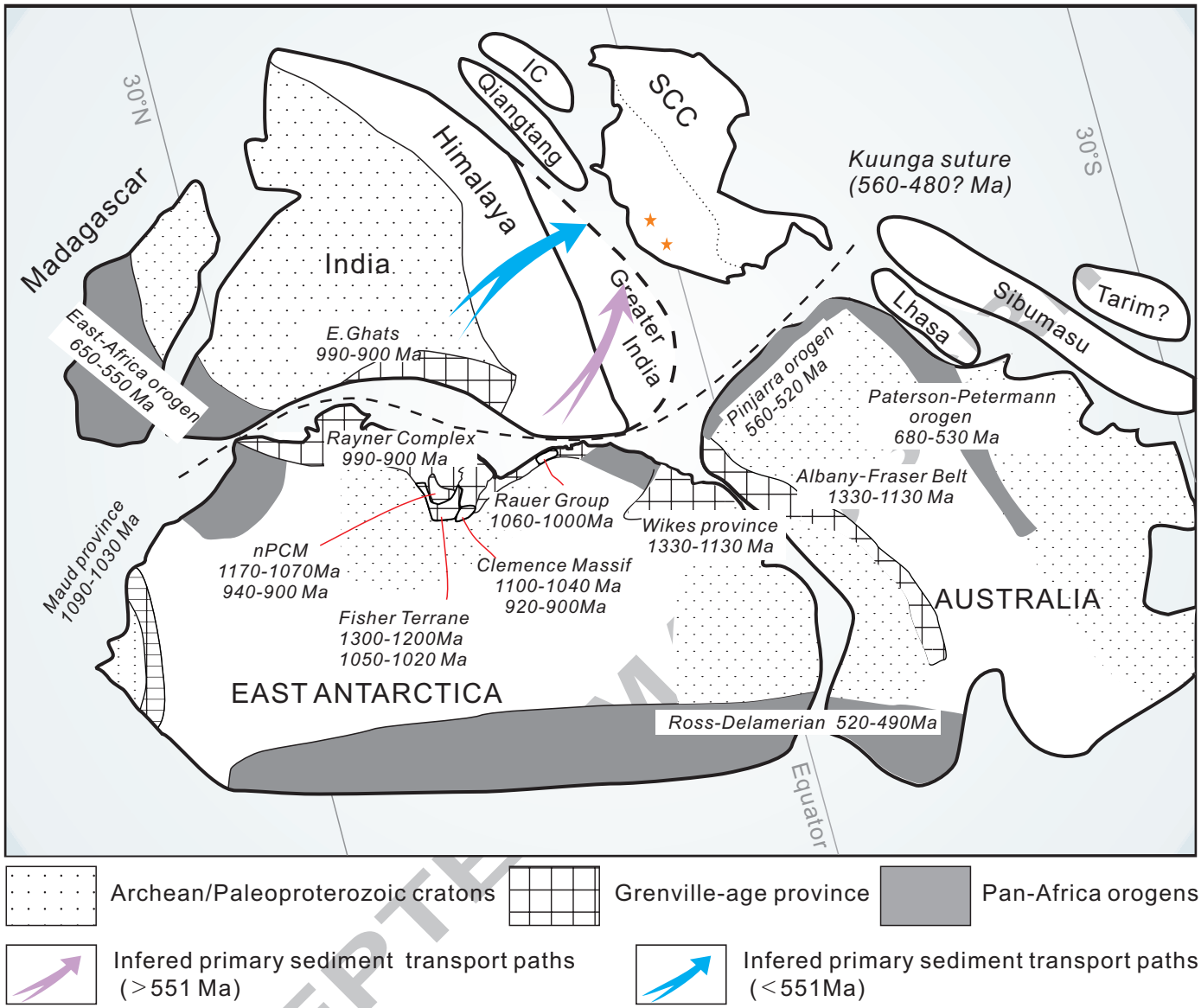

Archean/Paleoproterozoic cratons

Grenville-age province

Pan-Africa orogens

Infered primary sediment transport paths (>551 Ma)

Infered primary sediment transport paths (<551Ma)

Fig. 12